Mitochondrial respiratory states and rates:
Building blocks of mitochondrial physiology
Part 1.

MitoEAGLE Network

Corresponding author: Gnaiger E

Contributing co-authors

Ahn B, Alves MG, Amati F, Aral C, Arandarčikaitė O, Åsander Frostner E, Bailey DM, Bastos Sant'Anna Silva AC, Battino M, Beard DA, Ben-Shachar D, Bishop D, Breton S, Brown GC, Brown RA, Buettner GR, Calabria E, Cardoso LHD, Carvalho E, Casado Pinna M, Cervinkova Z, Chang SC, Chicco AJ, Chinopoulos C, Coen PM, Collins JL, Crisóstomo L, Davis MS, Dias T, Distefano G, Doerrier C, Drahota Z, Duchen MR, Ehinger J, Elmer E, Endlicher R, Fell DA, Ferko M, Ferreira JCB, Filipovska A, Fisar Z, Fisher J, Garcia-Roves PM, Garcia-Souza LF, Genova ML, Gonzalo H, Goodpaster BH, Gorr TA, Grefte S, Han J, Harrison DK, Hellgren KT, Hernansanz P, Holland O, Hoppel CL, Houstek J, Hunger M, Iglesias-Gonzalez J, Irving BA, Iyer S, Jackson CB, Jansen-Dürr P, Jespersen NR, Jha RK, Kaambre T, Kane DA, Kappler L, Karabatsiakis A, Keijer J, Keppner G, Komlodi T, Kopitar-Jerala N, Krako Jakovljevic N, Kuang J, Kucera O, Labieniec-Watala M, Lai N, Laner V, Larsen TS, Lee HK, Lemieux H, Lerfall J, Lucchinetti E, MacMillan-Crow LA, Makrecka-Kuka M, Meszaros AT, Michalak S, Moisoi N, Molina AJA, Montaigne D, Moore AL, Moreira BP, Mracek T, Muntane J, Muntean DM, Murray AJ, Nedergaard J, Nemec M, Newsom S, Nozickova K, O'Gorman D, Oliveira PF, Oliveira PJ, Orynbayeva Z, Pak YK, Palmeira CM, Patel HH, Pecina P, Pereira da Silva Grilo da Silva F, Pesta D, Petit PX, Pichaud N, Pirkmajer S, Porter RK, Pranger F, Prochownik EV, Puurand M, Radenkovic F, Reboredo P, Renner-Sattler K, Robinson MM, Rohlena J, Røsland GV, Rossiter HB, Rybacka-Mossakowska J, Saada A, Salvadego D, Scatena R, Schartner M, Scheibye-Knudsen M, Schilling JM, Schlattner U, Schoenfeld P, Scott GR, Shabalina IG, Sharma P, Shevchuk I, Siewiera K, Singer D, Sobotka O, Spinazzi M, Stankova P, Stier A, Stocker R, Sumbalova Z, Suravajhala P, Tanaka M, Tandler B, Tepp K, Tomar D, Towheed A, Tretter L, Trivigno C, Tronstad KJ, Trougakos IP, Tyrrell DJ, Urban T, Velika B, Vendelin M, Vercesi AE, Victor VM, Villena JA, Wagner BA, Ward ML, Watala C, Wei YH, Wieckowski MR, Wohlwend M, Wolff J, Wuest RCI, Zaugg K, Zaugg M, Zorzano A

Supporting co-authors:

Bakker BM, Bernardi P, Boetker HE, Borsheim E, Borutaitė V, Bouitbir J, Calbet JA, Calzia E, Chaurasia B, Clementi E, Coker RH, Collin A, Das AM, De Palma C, Dubouchaud H, Durham WJ, Dyrstad SE, Engin AB, Fornaro M, Gan Z, Garlid KD, Garten A, Gourlay CW, Granata C, Haas CB, Haavik J, Haendeler J, Hand SC, Hepple RT, Hickey AJ, Hoel F, Jang DH, Kainulainen H, Khamoui AV, Klingenspor M, Koopman WJH, Kowaltowski AJ, Krajcova A, Lane N, Lenaz G, Malik A, Markova M, Mazat JP, Menze MA, Methner A, Neuzil J, Oliveira MT, Pallotta ML, Parajuli N, Pettersen IKN, Porter C, Pulinilkunnil T, Ropelle ER, Salin K, Sandi C, Sazanov LA, Silber AM, Skolik R, Smenes BT, Soares FAA, Sokolova I, Sonkar VK, Swerdlow RH, Szabo I, Trifunovic A, Thyfault JP, Valentine JM, Vieyra A, Votion DM, Williams C, Zischka H

Updates and discussion:

Correspondence: Gnaiger E

Department of Visceral, Transplant and Thoracic Surgery, D. Swarovski Research Laboratory, Medical University of Innsbruck, Innrain 66/4, A-6020 Innsbruck, Austria

Email: erich.gnaiger@i-med.ac.at

Tel: +43 512 566796, Fax: +43 512 566796 20

*This manuscript on 'Mitochondrial respiratory states and rates' is a position statement in the frame of COST Action CA15203 MitoEAGLE. The list of co-authors evolved beyond **phase 1** (phase 1 versions 1 – 44) in the **bottom-up** spirit of COST.*

This is an open invitation to scientists and students to join as co-authors, to provide a balanced view on mitochondrial respiratory control and a consensus statement on reporting data of mitochondrial respiration in terms of metabolic flows and fluxes.

Mitochondrial fitness mapping - Quality management network

***Phase 2:** MitoEAGLE preprint 'The protonmotive force and respiratory control' (Versions 01 – 21): We continue to invite comments and suggestions, particularly if you are an **early career investigator adding an open future-oriented perspective**, or an **established scientist providing a balanced historical basis**. Your critical input into the quality of the manuscript will be most welcome, improving our aims to be educational, general, consensus-oriented, and practically helpful for students working in mitochondrial respiratory physiology.*

2017-11-11: Print version forMiP2017 and MitoEAGLE workshop in Hradec Kralove:

» http://www.mitoeagle.org/index.php/MiP2017_Hradec_Kralove_CZ

***Phase 3** (Versions 22 –)**: Discussion of manuscript submission to a preprint server—such as BioRxiv; invite further opinion leaders:** To join as a co-author, please feel free to focus on a particular section, providing direct input and references, and contributing to the scope of the manuscript from the perspective of your expertise. Your comments will be largely posted on the discussion page of the MitoEAGLE preprint website.*

If you prefer to submit comments in the format of a referee's evaluation rather than a contribution as a co-author, I will be glad to distribute your views to the updated list of co-authors for a balanced response. We would ask for your consent on this open bottom-up policy.

***Phase 4**: Journal submission. We plan a series of follow-up reports by the expanding MitoEAGLE Network, to increase the scope of recommendations on harmonization and facilitate global communication and collaboration. Further discussions: MitoEAGLE Working Group Meetings, various conferences (EBEC 2018 in Budapest).*

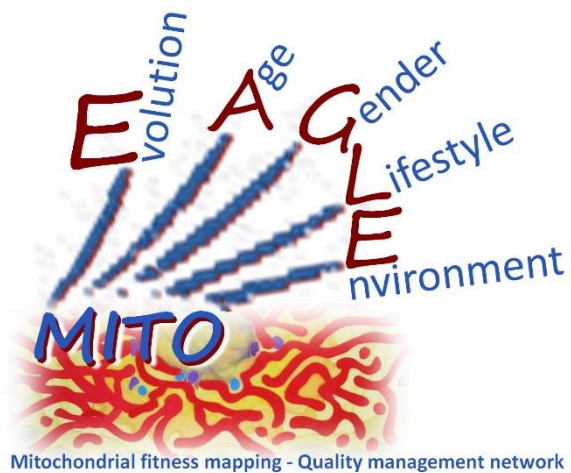*» http://www.mitoglobal.org/index.php/EBEC2018_Budapest_HU*

I thank you in advance for your feedback.

With best wishes,

Erich Gnaiger

Chair Mitochondrial Physiology Society – http://www.mitophysiology.org
Chair COST Action MitoEAGLE – http://www.mitoeagle.org

Contents

Abstract As the knowledge base and importance of mitochondrial physiology to human health expand, the necessity for harmonizing nomenclature concerning mitochondrial respiratory states and rates has become increasingly apparent. Clarity of concept and consistency of nomenclature are key trademarks of a research field. These trademarks facilitate effective transdisciplinary communication, education, and ultimately further discovery. Peter Mitchell's chemiosmotic theory establishes the link between vectorial and scalar energy transformation and coupling in oxidative phosphorylation. The unifying concept of the protonmotive force provides the framework for developing a consistent theory and nomenclature for mitochondrial physiology and bioenergetics. Herein, we follow IUPAC guidelines on general terms of physical chemistry, extended by considerations on open systems and irreversible thermodynamics. We align the nomenclature and symbols of classical bioenergetics with a concept-driven constructive terminology to express the meaning of each quantity clearly and consistently. In this position statement, in the frame of COST Action MitoEAGLE, we endeavour to provide a balanced view on mitochondrial respiratory control and a critical discussion on reporting data of mitochondrial respiration in terms of metabolic flows and fluxes. Uniform standards for evaluation of respiratory states and rates will ultimately support the development of databases of mitochondrial respiratory function in species, tissues, and cells.

Keywords: Mitochondrial respiratory control, coupling control, mitochondrial preparations, protonmotive force, oxidative phosphorylation, OXPHOS, efficiency, electron transfer, ET; proton leak, LEAK, residual oxygen consumption, ROX, State 2, State 3, State 4, normalization, flow, flux

Executive summary

See:

http://www.mitoeagle.org/index.php/MitoEAGLE_preprint_2018-02-08#Executive_summary

Box 1: In brief – Mitochondria and Bioblasts

Mitochondria are the oxygen-consuming electrochemical generators which evolved from endosymbiotic bacteria (Margulis 1970; Lane 2005). They were described by Richard Altmann (1894) as 'bioblasts', which include not only the mitochondria as presently defined, but also symbiotic and free-living bacteria. The word 'mitochondria' (Greek mitos: thread; chondros: granule) was introduced by Carl Benda (1898).

Mitochondrial dysfunction is associated with a wide variety of genetic and degenerative diseases. Robust mitochondrial function is supported by physical exercise and caloric balance, and is central for sustained metabolic health throughout life. Therefore, a more consistent presentation of mitochondrial physiology will improve our understanding of the etiology of disease, the diagnostic repertoire of mitochondrial medicine, with a focus on protective medicine, lifestyle and healthy aging.

We now recognize mitochondria as dynamic organelles with a double membrane that are contained within eukaryotic cells. The mitochondrial inner membrane (mtIM) shows dynamic tubular to disk-shaped cristae that separate the mitochondrial matrix, *i.e.*, the negatively charged internal mitochondrial compartment, and the intermembrane space; the latter being positively charged and enclosed by the mitochondrial outer membrane (mtOM). The mtIM contains the non-bilayer phospholipid cardiolipin, which is not present in any other eukaryotic cellular membrane. Cardiolipin promotes the formation of respiratory supercomplexes, which are supramolecular assemblies based upon specific, though dynamic, interactions between individual respiratory complexes (Greggio *et al.* 2017; Lenaz *et al.* 2017). Membrane fluidity exters an influence on functional properties of proteins incorporated in the membranes (Waczulikova *et al.* 2007).

Mitochondria are the structural and functional elements of cell respiration. Cell respiration is the consumption of oxygen by electron transfer coupled to electrochemical proton translocation across the mtIM. In the process of oxidative phosphorylation (OXPHOS), the reduction of O_2 is electrochemically coupled to the transformation of energy in the form of adenosine triphosphate (ATP; Mitchell 1961, 2011). Mitochondria are the powerhouses of the cell which contain the machinery of the OXPHOS-pathways, including transmembrane respiratory complexes—proton pumps with FMN, Fe-S and cytochrome *b*, *c*, aa_3 redox systems); alternative dehydrogenases and oxidases; the coenzyme ubiquinone (Q); F-ATPase or ATP synthase; the enzymes of the tricarboxylic acid cycle and the fatty acid oxidation enzymes; transporters of ions, metabolites and co-factors; and mitochondrial kinases related to energy transfer pathways. The mitochondrial proteome comprises over 1,200 proteins (Calvo *et al.* 2015; 2017), mostly encoded by nuclear DNA (nDNA), with a variety of functions, many of which are relatively well known (*e.g.,* apoptosis-regulating proteins), while others are still under investigation, or need to be identified (*e.g.,* alanine transporter).

There is a constant crosstalk between mitochondria and the other cellular components, maintaining cellular mitostasis through regulation at both the transcriptional and post-translational level, and through cell signalling including proteostatic (*e.g.*, the ubiquitin-proteasome and autophagy-lysosome pathways) and genome stability modules throughout the cell cycle or even cell death, contributing to homeostatic regulation in response to varying energy demands and stress (Quiros *et al.* 2016). In addition to mitochondrial movement along the microtubules, mitochondrial morphology can change in response to energy requirements of the cell via processes known as fusion and fission, through which mitochondria communicate within a network, and in response to intracellular stress factors causing swelling and ultimately permeability transition.

Mitochondria typically maintain several copies of their own genome (hundred to thousands per cell; Cummins 1998), which is maternally inherited (White *et al.* 2008) and

known as mitochondrial DNA (mtDNA). One exception to strictly maternal inheritance in animals is found in bivalves (Breton *et al.* 2007). mtDNA is 16.5 kB in length, contains 13 protein-coding genes for subunits of the transmembrane respiratory Complexes CI, CIII, CIV and F-ATPase, and also encodes 22 tRNAs and the mitochondrial 16S and 12S rRNA. Additional gene content is encoded in the mitochondrial genome, *e.g.,* microRNAs, piRNA, smithRNAs, repeat associated RNA, and even additional proteins (Duarte *et al.* 2014; Lee *et al.* 2015; Cobb *et al.* 2016). The mitochondrial genome is both regulated and supplemented by nuclear-encoded mitochondrial targeted proteins.

Abbreviation: mt, as generally used in mtDNA. Mitochondrion is singular and mitochondria is plural.

'*For the physiologist, mitochondria afforded the first opportunity for an experimental approach to structure-function relationships, in particular those involved in active transport, vectorial metabolism, and metabolic control mechanisms on a subcellular level*' (Ernster and Schatz 1981).

---

1. Introduction

Mitochondria are the powerhouses of the cell with numerous physiological, molecular, and genetic functions (**Box 1**). Every study of mitochondrial function and disease is faced with **E**volution, **A**ge, **G**ender and sex, **L**ifestyle, and **E**nvironment (EAGLE) as essential background conditions intrinsic to the individual patient or subject, cohort, species, tissue and to some extent even cell line. As a large and highly coordinated group of laboratories and researchers, the mission of the global MitoEAGLE Network is to generate the necessary scale, type, and quality of consistent data sets and conditions to address this intrinsic complexity. Harmonization of experimental protocols and implementation of a quality control and data management system are required to interrelate results gathered across a spectrum of studies and to generate a rigorously monitored database focused on mitochondrial respiratory function. In this way, researchers within the same and across different disciplines will be positioned to compare findings across traditions and generations to an agreed upon set of clearly defined and accepted international standards.

Reliability and comparability of quantitative results depend on the accuracy of measurements under strictly-defined conditions. A conceptual framework is required to warrant meaningful interpretation and comparability of experimental outcomes carried out by research groups at different institutes. With an emphasis on quality of research, collected data can be useful far beyond the specific question of a particular experiment. Enabling meta-analytic studies is the most economic way of providing robust answers to biological questions (Cooper *et al.* 2009). Vague or ambiguous jargon can lead to confusion and may relegate valuable signals to wasteful noise. For this reason, measured values must be expressed in standardized units for each parameter used to define mitochondrial respiratory function. Standardization of nomenclature and definition of technical terms are essential to improve the awareness of the intricate meaning of current and past scientific vocabulary, for documentation and integration into databases in general, and quantitative modelling in particular (Beard 2005). The focus on coupling states and fluxes through metabolic pathways of aerobic energy transformation in mitochondrial preparations is a first step in the attempt to generate a harmonized and conceptually-oriented nomenclature in bioenergetics and mitochondrial physiology. Coupling states of intact cells, the protonmotive force, and respiratory control by fuel substrates and specific inhibitors of respiratory enzymes will be reviewed in subsequent communications.
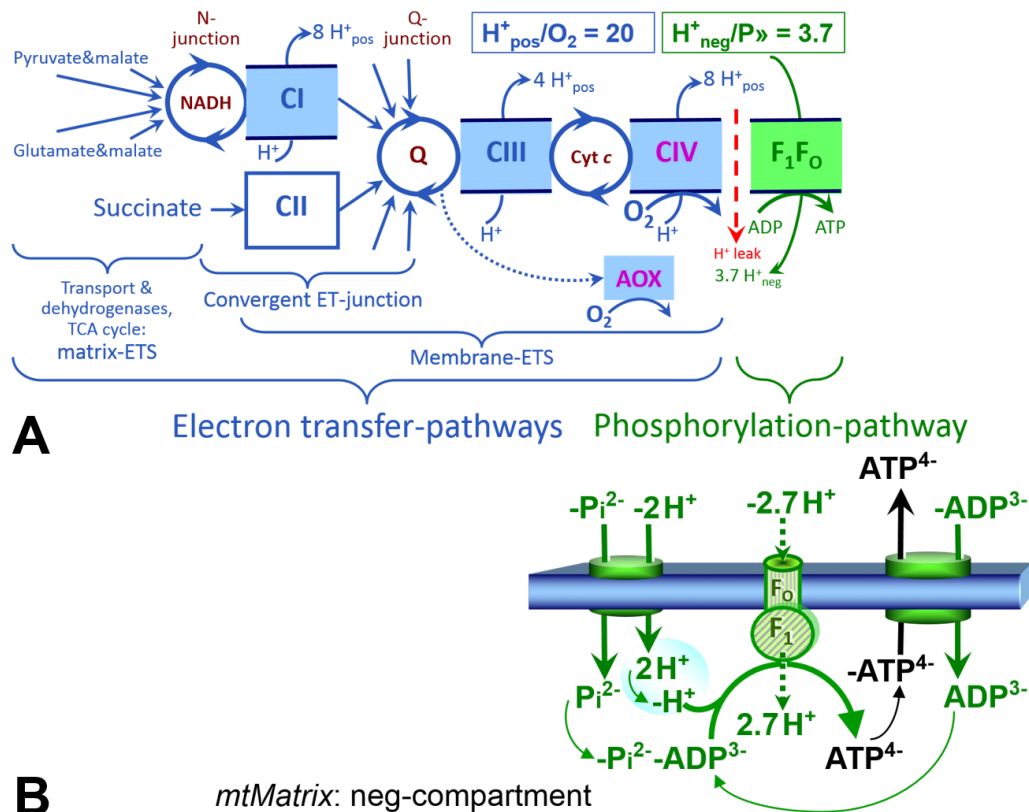
2. Oxidative phosphorylation and coupling states in mitochondrial preparations

'Every professional group develops its own technical jargon for talking about matters of critical concern ... People who know a word can share that idea with other members of their group, and a shared vocabulary is part of the glue that holds people together and allows them to create a shared culture' (Miller 1991).

Mitochondrial preparations are defined as either isolated mitochondria, or tissue and cellular preparations in which the barrier function of the plasma membrane is disrupted. The plasma membrane separates the cytosol, nucleus, and organelles (the intracellular compartment) from the environment of the cell. The plasma membrane consists of a lipid bilayer, embedded proteins, and attached organic molecules that collectively control the selective permeability of ions, organic molecules, and particles across the cell boundary. The intact plasma membrane, therefore, prevents the passage of many water-soluble mitochondrial substrates—such as succinate or adenosine diphosphate (ADP), that are required for the analysis of respiratory capacity at kinetically-saturating concentrations; this limits the scope of investigations into mitochondrial respiratory function in intact cells. The cholesterol content of the plasma membrane is high compared to mitochondrial membranes. Therefore, mild detergents—such as digitonin and saponin—can be applied to selectively permeabilize the plasma membrane by interaction with cholesterol and allow free exchange of cytosolic components with ions and organic molecules of the immediate cell environment, while maintaining the integrity and localization of organelles, cytoskeleton, and the nucleus. Application of optimum concentrations of permeabilization agents (mild detergents or toxins) leads to the complete loss of cell viability, tested by nuclear staining and washout of cytosolic marker enzymes—such as lactate dehydrogenase, while mitochondrial function remains intact. The respiration rate of isolated mitochondria remains unaltered after the addition of low concertations of digitonin or saponin. In addition to mechanical permeabilization during homogenization of tissue, peremeabilization agents may be applied to ensure permeabilization of all cells. Suspensions of cells permeabilized in the respiration chamber and crude tissue homogenates contain all components of the cell at highly diluted concentrations. All mitochondria are retained in chemically-permeabilized mitochondrial preparations and crude tissue homogenates. In the preparation of isolated mitochondria, the cells or tissues are homogenized, and the mitochondria are separated from other cell fractions and purified by differential centrifugation, entailing the loss of a fraction of mitochondria. Typical mitochondrial recovery ranges from 30% to 80%. Maximization of the purity of isolated mitochondria may compromise not only the mitochondrial yield but also the structural and functional integrity. Therefore, protocols for isolation of mitochondria need to be optimized according to the relevant questions addressed in a study. The term mitochondrial preparation does not include further fractionation of mitochondrial components, as well as submitochondrial particles.

2.1. Three coupling states of mitochondrial preparations and residual oxygen consumption

Respiratory capacities in coupling control states: To extend the classical nomenclature on mitochondrial coupling states (Section 2.3) by a concept-driven terminology that incorporates explicitly information on the nature of respiratory states, the terminology must be general and not restricted to any particular experimental protocol or mitochondrial preparation (Gnaiger 2009). We focus primarily on the conceptual 'why', along with clarification of the experimental 'how'. In the following section, the concept-driven terminology is explained and coupling states are defined. We define respiratory capacities, comparable to channel capacity in information theory (Schneider 2006), as the upper bound of the rate of respiration measured in defined coupling control states and electron transfer-pathway (ET-pathway) states.

Fig. 1. The oxidative phosphorylation (OXPHOS) system. (A) The mitochondrial electron transfer system (ETS) is fuelled by diffusion and transport of substrates across the mtOM and mtIM and consists of the matrix-ETS and membrane-ETS. Electron transfer (ET) pathways are coupled to the phosphorylation-pathway. ET-pathways converge at the N-junction and Q-junction (additional arrows indicate electron entry into the Q-junction through electron transferring flavoprotein, glycerophosphate dehydrogenase, dihydro-orotate dehydrogenase, choline dehydrogenase, and sulfide-ubiquinone oxidoreductase). The dotted arrow indicates the branched pathway of oxygen consumption by alternative quinol oxidase (AOX). The H^+_{pos}/O_2 ratio is the outward proton flux from the matrix space to the positively (pos) charged compartment, divided by catabolic O_2 flux in the NADH-pathway. The $H^+_{neg}/P»$ ratio is the inward proton flux from the inter-membrane space to the negatively (neg) charged matrix space, divided by the flux of phosphorylation of ADP to ATP (Eq. 1). Due to ion leaks and proton slip these are not fixed stoichiometries. **(B)** Phosphorylation-pathway catalyzed by the proton pump F_1F_O-ATPase, adenine nucleotide translocase, and inorganic phosphate transporter. The $H^+_{neg}/P»$ stoichiometry is the sum of the coupling stoichiometry in the F-ATPase reaction (-2.7 H^+_{pos} from the positive intermembrane space, 2.7 H^+_{neg} to the matrix, *i.e.*, the negative compartment) and the proton balance in the translocation of ADP^{2-}, ATP^{3-} and P_i^{2-}. Modified from (A) Lemieux *et al*. (2017) and (B) Gnaiger (2014).

To provide a diagnostic reference for respiratory capacities of core energy metabolism, the capacity of *oxidative phosphorylation*, OXPHOS, is measured at kinetically-saturating concentrations of ADP and inorganic phosphate, P_i. The *oxidative* ET-capacity reveals the limitation of OXPHOS-capacity mediated by the *phosphorylation*-pathway. The ET- and phosphorylation-pathways comprise coupled segments of the OXPHOS-system. ET-capacity is measured as noncoupled respiration by application of *external uncouplers*. The contribution of *intrinsically uncoupled* oxygen consumption is most easily studied in the absence of ADP—by not stimulating phosphorylation, or by inhibition of the phosphorylation-pathway. The corresponding states are collectively classified as LEAK-states, when oxygen consumption

358 compensates mainly for ion leaks including the proton leak (**Table 1**). Defined coupling states
359 are induced by: (*1*) adding cation chelators such as EGTA, binding free Ca^{2+} and thus limiting
360 cation cycling; (*2*) adding ADP and P_i; (*3*) inhibiting the phosphorylation-pathway; and (*4*)
361 uncoupler titrations, while maintaining a defined ET-pathway state with constant fuel substrates
362 and inhibitors of specific branches of the ET-pathway (**Fig. 1**).

Table 1. Coupling states and residual oxygen consumption in mitochondrial preparations in relation to respiration- and phosphorylation-rate, J_{kO_2} and $J_{P»}$, and protonmotive force, pmf. Coupling states are established at kinetically-saturating concentrations of fuel substrates and O_2.

| State	J_{kO_2}	$J_{P»}$	pmf	Inducing factors	Limiting factors
LEAK	L; low, cation leak-dependent respiration	0	max.	proton leak, slip, and cation cycling	$J_{P»} = 0$: (*1*) without ADP, L_N; (*2*) max. ATP/ADP ratio, L_T; or (*3*) inhibition of the phosphorylation-pathway, L_{Omy}
OXPHOS	P; high, ADP-stimulated respiration	max.	high	kinetically-saturating [ADP] and [P_i]	$J_{P»}$ by phosphorylation-pathway; or J_{kO_2} by ET-capacity
ET	E; max., noncoupled respiration	0	low	optimal external uncoupler concentration for max. $J_{O_2,E}$	J_{kO_2} by ET-capacity
ROX	*Rox*; min., residual O_2 consumption	0	0	$J_{O_2,Rox}$ in non-ET-pathway oxidation reactions	full inhibition of ET-pathway; or absence of fuel substrates

369 **Kinetic control:** Coupling control states are established in the study of mitochondrial
370 preparations to obtain reference values for various output variables. Physiological conditions *in*
371 *vivo* deviate from these experimentally obtained states. Since kinetically-saturating
372 concentrations, *e.g.,* of ADP or oxygen, may not apply to physiological intracellular conditions,
373 relevant information is obtained in studies of kinetic responses to conditions intermediate
374 between the LEAK state at zero [ADP] and the OXPHOS-state at saturating [ADP], or of
375 respiratory capacities in the range between kinetically-saturating [O_2] and anoxia (Gnaiger
376 2001).
377 **The steady-state:** Mitochondria represent a thermodynamically open system in non-
378 equilibrium states of biochemical energy transformation. State variables (protonmotive force;
379 redox states) and metabolic *rates* (fluxes) are measured in defined mitochondrial respiratory
380 *states*. Strictly, steady states can be obtained only in open systems, in which changes by *internal*
381 transformations, *e.g.*, O_2 consumption, are instantaneously compensated for by *external* fluxes,
382 *e.g.*, O_2 supply, preventing a change of oxygen concentration in the system (Gnaiger 1993b).
383 Mitochondrial respiratory states monitored in closed systems satisfy the criteria of pseudo-
384 steady states for limited periods of time, when changes in the system (concentrations of O_2,
385 fuel substrates, ADP, P_i, H^+) do not exert significant effects on metabolic fluxes (respiration,
386 phosphorylation). Such pseudo-steady states require respiratory media with sufficient buffering
387 capacity and kinetically-saturating concentrations of substrates to be maintained, and thus
388 depend on the kinetics of the processes under investigation.

389   **Specification of biochemical dose:** Substrates, uncouplers, inhibitors, and other
390   biochemical reagents are titrated to dissect mitochondrial function. Nominal concentrations of
391   these substances are usually reported as initial amount of substance concentration [$mol \cdot L^{-1}$] in
392   the incubation medium. When aiming at the measurement of kinetically saturated processes—
393   such as OXPHOS-capacities, the concentrations for substrates can be chosen according to the
394   apparent equilibrium constant, K_m'. In the case of hyperbolic kinetics, only 80% of maximum
395   respiratory capacity is obtained at a substrate concentration of four times the K_m', whereas
396   substrate concentrations of 5, 9, 19 and 49 times the K_m' are theoretically required for reaching
397   83%, 90%, 95% or 98% of the maximal rate (Gnaiger 2001). Other reagents are chosen to
398   inhibit or alter some process. The amount of these chemicals in an experimental incubation is
399   selected to maximize effect, yet not lead to unacceptable off-target consequences that would
400   adversely affect the data being sought. Specifying the amount of substance in an incubation as
401   nominal concentration in the aqueous incubation medium can be ambiguous (Doskey *et al*.
402   2015), particularly when lipophilic substances (oligomycin; uncouplers, permeabilization
403   agents) or cations (TPP^+; fluorescent dyes such as safranin, TMRM) are applied which
404   accumulate in biological membranes or the mitochondrial matrix. For example, a dose of
405   digitonin of 8 $fmol \cdot cell^{-1}$ (10 $\mu g \cdot 10^{-6}$ cells) is optimal for permeabilization of endothelial cells,
406   and the concentration in the incubation medium has to be adjusted according to the cell density
407   applied (Doerrier *et al*. 2018). Generally, dose/exposure can be specified per unit of biological
408   sample, *i.e.*, (nominal moles of xenobiotic)/(number of cells) [$mol \cdot cell^{-1}$] or, as appropriate, per
409   mass of biological sample [$mol \cdot kg^{-1}$]. This approach to specification of dose/exposure provides
410   a scalable parameter that can be used to design experiments, help interpret a wide variety of
411   experimental results, and provide absolute information that allows researchers worldwide to
412   make the most use of published data (Doskey *et al*. 2015).

413   **Phosphorylation, P»:** *Phosphorylation* in the context of OXPHOS is defined as
414   phosphorylation of ADP by P_i to ATP. On the other hand, the term phosphorylation is used
415   generally in many contexts, *e.g.,* protein phosphorylation. This justifies consideration of a
416   symbol more discriminating and specific than P as used in the P/O ratio (phosphate to atomic
417   oxygen ratio; O = 0.5 O_2), where P indicates phosphorylation of ADP to ATP or GDP to GTP.
418   We propose the symbol P» for the endergonic (uphill) direction of phosphorylation
419   ADP→ATP, and likewise the symbol P« for the corresponding exergonic (downhill) hydrolysis
420   ATP→ADP (**Fig. 2**). P» refers mainly to electrontransfer phosphorylation but may also involve
421   substrate-level phosphorylation as part of the tricarboxylic acid cycle (succinyl-CoA ligase)
422   and phosphorylation of ADP catalyzed by phosphoenolpyruvate carboxykinase.
423   Transphosphorylation is performed by adenylate kinase, creatine kinase, hexokinase and
424   nucleoside diphosphate kinase. In isolated mammalian mitochondria ATP production catalyzed
425   by adenylate kinase, 2 ADP ↔ ATP + AMP, proceeds without fuel substrates in the presence
426   of ADP (Komlódi and Tretter 2017). Kinase cycles are involved in intracellular energy transfer
427   and signal transduction for regulation of energy flux.

428   **Coupling:** In mitochondrial electron transfer (**Fig. 1**), vectorial transmembrane proton
429   flux is coupled through the proton pumps CI, CIII and CIV to the catabolic flux of scalar
430   reactions, collectively measured as oxygen flux (**Fig. 2**). Thus mitochondria are elements of
431   energy transformation. Energy cannot be lost or produced in any internal process (First Law of
432   thermodynamics). Open and closed systems can gain or loose energy only by external fluxes—
433   by exchange with the environment. Energy is a conserved quantity. Therefore, energy can
434   neither be produced by mitochondria, nor is there any internal process without energy
435   conservation. Exergy is defined as the 'free energy' with the potential to perform work.
436   *Coupling* is the mechanistic linkage of an exergonic process (spontaneous, negative exergy
437   change) with an endergonic process (positive exergy change) in energy transformations which
438   conserve part of the exergy that would be irreversible lost or dissipated in an uncoupled process.
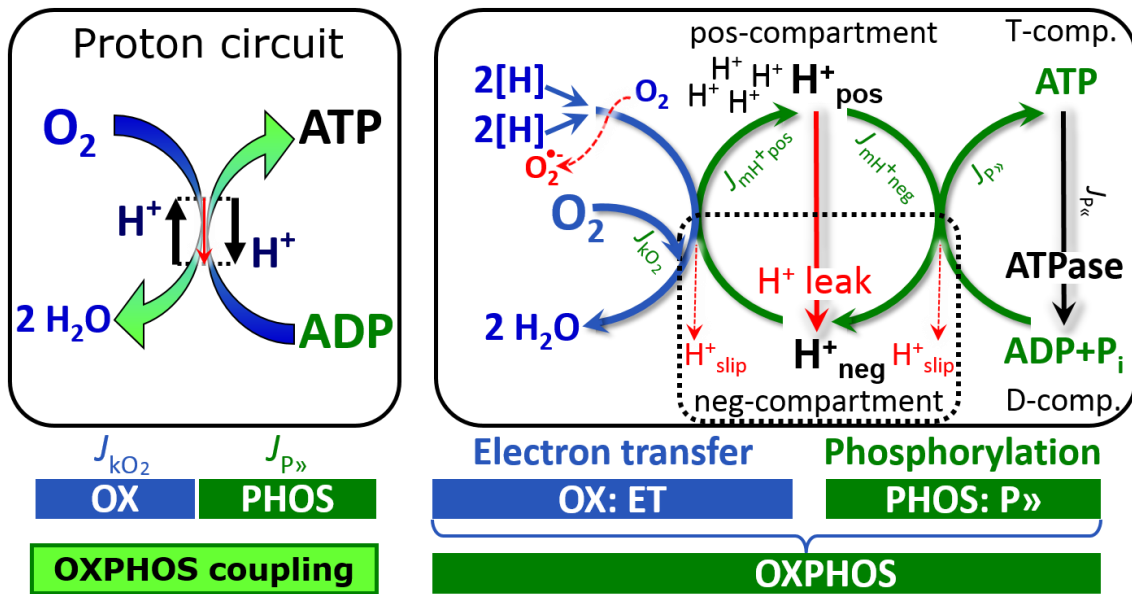
Fig. 2. The proton circuit and coupling in oxidative phosphorylation (OXPHOS). Oxygen flux, J_{kO_2}, through the catabolic ET-pathway, k, is coupled to flux through the phosphorylation-pathway of ADP to ATP, $J_{P»}$. The proton pumps of the ET-pathway drive proton flux into the positive (pos) compartment, J_{mH+pos}, which generates the output protonmotive force (motive, subscript m). F-ATPase is coupled to inward proton current into the negative (neg) compartment, J_{mH+neg}, to phosphorylate ADP+P_i to ATP. 2[H] indicates the reduced hydrogen equivalents of fuel substrates of the catabolic reaction k with oxygen. Fluxes are expressed per volume, V [m^3], of the system. The system defined by the boundaries (full black line) is not a black box, but is analysed as a compartmental system. The negative compartment (neg–compartment, enclosed by the dotted line) is the matrix space, separated by the mtIM from the positive compartment (pos–compartment). ADP+P_i and ATP are the substrate- and product–compartments (scalar ADP and ATP compartments, D–comp. and T–comp.), respectively. At steady-state proton turnover, $J_{\infty H+}$, and ATP turnover, $J_{\infty P}$, maintain concentrations constant, when $J_{mH+\infty} = J_{mH+pos} = J_{mH+neg}$, and $J_{P\infty} = J_{P»} = J_{P«}$. Modified from Gnaiger (2014).

Uncoupling: Uncoupling is a general term comprising diverse mechanisms. Differences of terms—uncoupled *vs.* noncoupled—are easily overlooked, although they relate to different mechanisms of uncoupling (**Fig. 3**). An attempt at rigorous definition is required for clarification of concepts (**Table 2**).

1. Proton leak across the mtIM from the pos– to the neg–compartment (**Fig. 2**);
2. Cycling of other cations, strongly stimulated by permeability transition;
3. Proton slip in the proton pumps when protons are effectively not pumped (CI, CIII and CIV) or are not driving phosphorylation (F-ATPase);
4. Loss of compartmental integrity when electron transfer is acoupled;
5. Electron leak in the loosely coupled univalent reduction of oxygen (O$_2$; dioxygen) to superoxide anion radical (O$_2^{\bullet-}$).
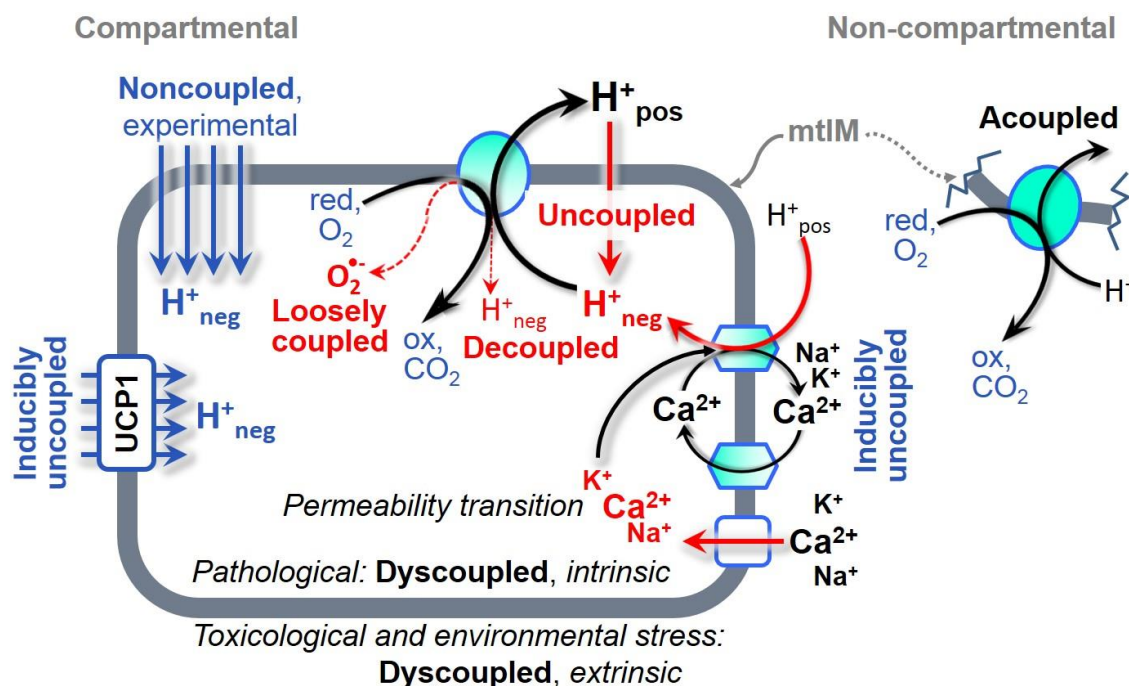
Fig 3. Mechanisms of respiratory uncoupling. An intact mitochondrial inner membrane, mtIM, is required for vectorial, compartmental coupling. 'Acoupled' respiration is the consequence of structural disruption with catalytic activity of non-compartmental mitochondrial fragments. Inducibly uncoupled (activation of UCP1) and experimentally noncoupled respiration (titration of protonophores) stimulate respiration to maximum oxygen flux of ET-capacity. Uncoupled, decoupled, and loosely coupled respiration are components of intrinsic LEAK respiration. Pathological dysfunction may affect all types of uncoupling, including permeability transition, causing intrinsically dyscoupled respiration. Similarly, toxicological and environmental stress factors can cause extrinsically dyscoupled respiration.

LEAK-state (**Fig. 4**): The LEAK-state is defined as a state of mitochondrial respiration when O_2 flux mainly compensates for ion leaks in the absence of ATP synthesis, at kinetically-saturating concentrations of O_2 and respiratory fuel substrates. LEAK-respiration is measured to obtain an estimate of *intrinsic uncoupling* without addition of an experimental uncoupler: (*1*) in the absence of adenylates; (*2*) after depletion of ADP at a maximum ATP/ADP ratio; or (*3*) after inhibition of the phosphorylation-pathway by inhibitors of F-

Fig. 4. LEAK-state: Phosphorylation is arrested, $J_{P»} = 0$, and catabolic oxygen flux, $J_{kO_2,L}$, is controlled mainly by the proton leak, $J_{mH+neg,L}$, at maximum protonmotive force. See also **Fig. 2** and **3**.

ATPase—such as oligomycin, or of adenine nucleotide translocase—such as carboxyatractyloside. Adjustment of the nominal concentration of these inhibitors to the density of biological sample applied can minimize or avoid inhibitory side-effects exerted on ET-capacity or even some dyscoupling.
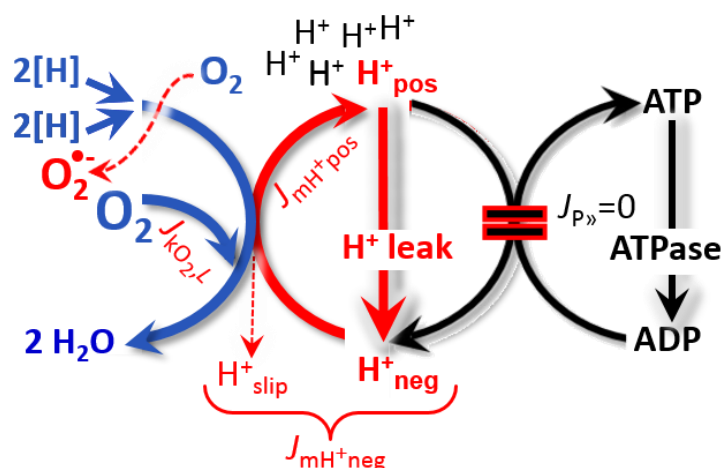
Table 2. Distinction of terms related to coupling and uncoupling (Fig. 3).

Term	Respiration	P»/O$_2$	Note
Acoupled		0	electron transfer in mitochondrial fragments without vectorial proton translocation
Uncoupled	*L*	0	non-phosphorylating intrinsic LEAK-respiration, without added protonophore
uncoupled		0	component of LEAK-respiration, uncoupled *sui generis*, ion diffusion across the mtIM
Decoupled		0	component of LEAK-respiration, proton slip
loosely coupled		0	component of LEAK-respiration, lower coupling due to superoxide anion radical formation and bypass of proton pumps
Dyscoupled		0	pathologically, toxicologically, environmentally increased uncoupling, mitochondrial dysfunction
inducibly uncoupled	*E*	0	by UCP1 or cation (*e.g.*, Ca^{2+}) cycling
Noncoupled	*E*	0	non-phosphorylating respiration stimulated to maximum flux at optimum exogenous uncoupler concentration (**Fig. 6**)
well-coupled	*P*	high	phosphorylating respiration with an intrinsic LEAK component (**Fig. 5**)
fully coupled	*P − L*	max.	OXPHOS-capacity corrected for LEAK-respiration (**Fig. 7**)

Proton leak and uncoupled respiration: Proton leak is a leak current of protons. The intrinsic proton leak is the *uncoupled* process in which protons diffuse across the mtIM in the dissipative direction of the downhill protonmotive force without coupling to phosphorylation (**Fig. 4**). The proton leak flux depends non-linearly on the protonmotive force (Garlid *et al.* 1989; Divakaruni and Brand 2011), is a property of the mtIM, and may be enhanced due to possible contaminations by free fatty acids. Inducible uncoupling mediated by uncoupling protein 1 (UCP1) is physiologically controlled, *e.g.*, in brown adipose tissue. UCP1 is a member of the mitochondrial carrier family which is involved in the translocation of protons across the mtIM (Klingenberg 2017). As a consequence of this effective short-circuit, the protonmotive force diminishes, resulting in stimulation of electron transfer to O$_2$ and heat dissipation without phosphorylation of ADP.

Cation cycling: There can be other cation contributors to leak current including calcium and probably magnesium. Calcium current is balanced by mitochondrial Na$^+$/Ca^{2+} exchange, which is balanced by Na$^+$/H$^+$ exchange or K$^+$/H$^+$ exchange. This is another effective uncoupling mechanism different from proton leak.

Proton slip and decoupled respiration: Proton slip is the *decoupled* process in which protons are only partially translocated by a proton pump of the ET-pathways and slip back to the original compartment. The proton leak is the dominant contributor to the overall leak current in mammalian mitochondria incubated under physiological conditions at 37 °C, whereas proton slip is increased at lower experimental temperature (Canton *et al.* 1995). Proton slip can also happen in association with the F-ATPase, in which case the proton slips downhill across the pump to the matrix without contributing to ATP synthesis. In each case, proton slip is a property of the proton pump and increases with the turnover rate of the pump.

Electron leak and loosely coupled respiration: Superoxide anion radical production by the ETS leads to a bypass of proton pumps and correspondingly lower P»/O_2 ratio, which depends on the actual site of electron leak and the scavenging of hydrogen peroxide by cytochrome *c*, whereby electrons may re-enter the ETS with proton translocation by CIV.

Loss of compartmental integrity and acoupled respiration: Electron transfer and O_2 consumption proceed without compartmental proton translocation in disrupted mitochondrial fragments. Such fragments form during mitochondrial isolation, and may not fully fuse to re-establish structurally intact mitochondria. Loss of mtIM integrity, therefore, is the cause of acoupled respiration, which is a nonvectorial dissipative process without control by the protonmotive force.

Dyscoupled respiration: Mitochondrial injuries may lead to *dyscoupling* as a pathological or toxicological cause of *uncoupled* respiration. Dyscoupling may involve any type of uncoupling mechanism, *e.g.*, opening the permeability transition pore. Dyscoupled respiration is distinguished from the experimentally induced *noncoupled* respiration in the ET-state (**Fig. 3**).

OXPHOS-state (**Fig. 5**): The OXPHOS-state is defined as the respiratory state with kinetically-saturating concentrations of O_2, respiratory and phosphorylation substrates, and absence of exogenous uncoupler, which provides an estimate of the maximal respiratory capacity in the OXPHOS-state for any given ET-pathway state. Respiratory capacities at kinetically-saturating substrate concentrations provide reference values or upper limits of performance, aiming at the generation of data sets for

Fig. 5. OXPHOS-state: Phosphorylation, $J_{P»}$, is stimulated by kinetically-saturating [ADP] and inorganic phosphate, [P_i], and is supported by a high protonmotive force. O_2 flux, $J_{kO_2,P}$, is well-coupled at a P»/O_2 ratio of $J_{P»,P}/J_{O_2,P}$. See also **Fig. 2**.

comparative purposes. Physiological activities and effects of substrate kinetics can be evaluated relative to the OXPHOS-capacity.

As discussed previously, 0.2 mM ADP does not fully saturate flux in isolated mitochondria (Gnaiger 2001; Puchowicz *et al.* 2004); greater ADP concentration is required, particularly in permeabilized muscle fibres and cardiomyocytes, to overcome limitations by intracellular diffusion and by the reduced conductance of the mtOM (Jepihhina *et al.* 2011, Illaste *et al.* 2012, Simson *et al.* 2016), either through interaction with tubulin (Rostovtseva *et al.* 2008) or other intracellular structures (Birkedal *et al.* 2014). In permeabilized muscle fibre bundles of high respiratory capacity, the apparent K_m for ADP increases up to 0.5 mM (Saks *et al.* 1998), consistent with experimental evidence that >90% saturation is reached only at >5 mM ADP (Pesta and Gnaiger 2012). Similar ADP concentrations are also required for accurate determination of OXPHOS-capacity in human clinical cancer samples and permeabilized cells (Klepinin *et al.* 2016; Koit *et al.* 2017). Whereas 2.5 to 5 mM ADP is sufficient to obtain the actual OXPHOS-capacity in many types of permeabilized tissue and cell preparations, experimental validation is required in each specific case.
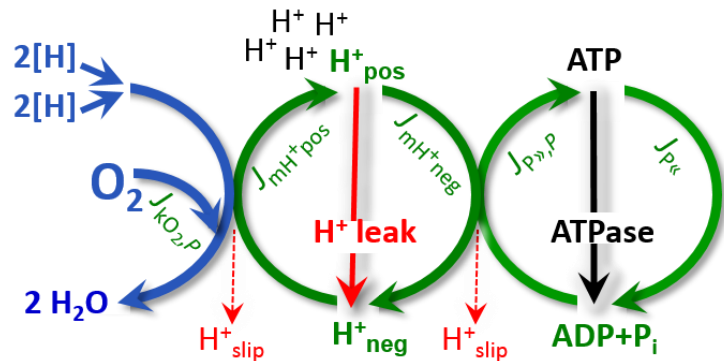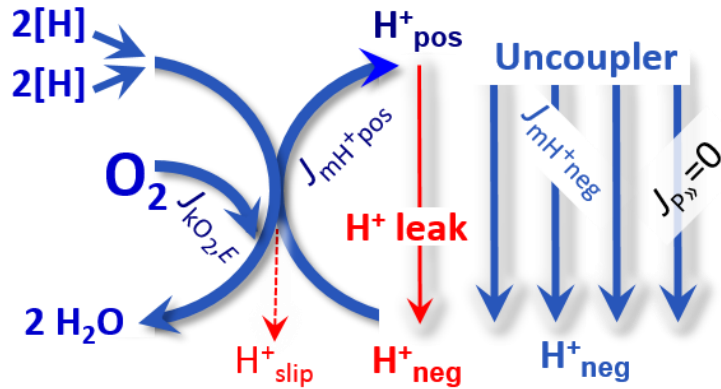
Electron transfer-state (**Fig. 6**): The ET-state is defined as the *noncoupled* state with kinetically-saturating concentrations of O_2, respiratory substrate and optimum *exogenous* uncoupler concentration for maximum O_2 flux, as an estimate of ET-capacity. Inhibition of respiration is observed at higher than optimum uncoupler concentrations. As a consequence of the nearly collapsed protonmotive force, the driving force is insufficient for phosphorylation, and $J_{P»} = 0$.

Fig. 6. ET-state: Noncoupled respiration, $J_{kO2,E}$, is maximum at optimum exogenous uncoupler concentration and phosphorylation is zero, $J_{P»} = 0$. See also **Fig. 2**.

Besides the three fundamental coupling states of mitochondrial preparations, the following respiratory state also is relevant to assess respiratory function:

ROX state and *Rox*: The rate of residual oxygen consumption, *Rox*, is defined as O_2 consumption due to oxidative side reactions remaining after inhibition of ET—with rotenone, malonic acid and antimycin A. Cyanide and azide not only inhibit CIV but several peroxidases which should be involved in *Rox*. ROX is not a coupling state. *Rox* represents a baseline that is used to correct mitochondrial respiration in defined coupling states. *Rox* is not necessarily equivalent to non-mitochondrial respiration, considering oxygen-consuming reactions in mitochondria not related to ET—such as oxygen consumption in reactions catalyzed by monoamine oxidases (type A and B), monooxygenases (cytochrome P450 monooxygenases), dioxygenase (sulfur dioxygenase and trimethyllysine dioxygenase), several hydoxylases, and more. Mitochondrial preparations, especially those obtained from liver, may be contaminated by peroxisomes. This fact makes the exact determination of mitochondrial oxygen consumption and mitochondria-associated generation of reactive oxygen species complicated (Schönfeld *et al.* 2009). The dependence of ROX-linked oxygen consumption needs to be studied in detail together with non-ET enzyme activities, availability of specific substrates, oxygen concentration, and electron leakage leading to the formation of reactive oxygen species.

2.2. Coupling states and respiratory rates

As an improvement of previous terminologies, we distinguish metabolic *pathways* from metabolic *states* and the corresponding metabolic *rates*; for example: ET-pathways (**Fig. 7**), ET-state (**Fig. 6**), and ET-capacity, *E*, respectively (**Table 1**). The protonmotive force is *high* in the OXPHOS-state when it drives phosphorylation, *maximum* in the LEAK-state of coupled mitochondria, driven by LEAK-respiration at a minimum back flux of cations to the matrix side, and *very low* in the ET-state when uncouplers short-circuit the proton cycle (**Table 1**).

The three coupling states, ET, LEAK and OXPHOS, are shown schematically with the corresponding respiratory rates, abbreviated as *E*, *L* and *P*, respectively (**Fig. 7**).

Fig. 7. Four-compartment model of oxidative phosphorylation. Respiratory states (ET, OXPHOS, LEAK) and corresponding rates (E, P, L) are connected by the protonmotive force, pmf. Electron transfer-capacity, E, is partitioned into (*1*) dissipative LEAK-respiration, L, when the Gibbs energy change of catabolic O_2 consumption is irreversibly lost, (*2*) net OXPHOS-capacity, P-L, with partial conservation of the capacity to perform work, and (*3*) the excess capacity, E-P. Modified from Gnaiger (2014).
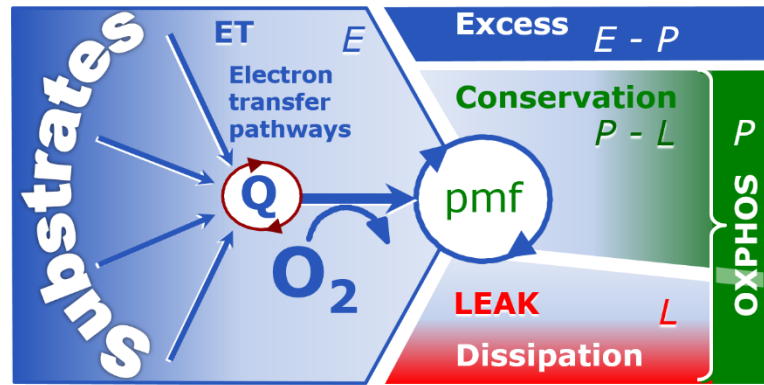
E may exceed or be equal to P. $E > P$ is observed in many types of mitochondria, varying between species, tissues and cell types (Gnaiger 2009). E-P is the excess ET-capacity pushing the phosphorylation-flux (**Fig. 1B**) to the limit of its *capacity of utilizing* the protonmotive force. In addition, the magnitude of E-P depends on the tightness of coupling or degree of uncoupling, since an increase of L causes P to increase towards the limit of E. The *excess E-P* capacity, E-P, therefore, provides a sensitive diagnostic indicator of specific injuries of the phosphorylation-pathway, under conditions when E remains constant but P declines relative to controls (**Fig. 7**). Substrate cocktails supporting simultaneous convergent electron transfer to the Q-junction for reconstitution of tricarboxylic acid cycle (TCA cycle or Krebs cycle) function establish pathway control states with high ET-capacity, and consequently increase the sensitivity of the E-P assay.

E cannot theoretically be lower than P. $E < P$ must be discounted as an artefact, which may be caused experimentally by: (*1*) loss of oxidative capacity during the time course of the respirometric assay, since E is measured subsequently to P; (*2*) using insuffient uncoupler concentrations; (*3*) using high uncoupler concentrations which inhibit ET (Gnaiger 2008); (*4*) high oligomycin concentrations applied for measurement of L before titrations of uncoupler, when oligomycin exerts an inhibitory effect on E. On the other hand, the excess ET-capacity is overestimated if non-saturating [ADP] or [P_i] are used. See State 3 in the next section.

P»/O_2 ratio: The P»/O_2 ratio (P»/4 e⁻) is two times the 'P/O' ratio (P»/2 e⁻) of classical bioenergetics. P»/O_2 is a generalized symbol, independent of measurement of phosphorylation by determination of P_i consumption (P_i/O_2 flux ratio), ADP depletion (ADP/O_2 flux ratio), or ATP production (ATP/O_2 flux ratio).

The mechanistic P»/O_2 ratio—or P»/O_2 stoichiometry—is calculated from the proton–to–oxygen and proton–to–phosphorylation coupling stoichiometries (**Fig. 1A**),

$$\text{P»}/O_2 \; = \; \frac{H^+_{pos}/O_2}{H^+_{neg}/\text{P»}} \tag{1}$$

The H^+_{pos}/O_2 *coupling stoichiometry* (referring to the full 4 electron reduction of O_2) depends on the ET-pathway control state which defines the relative involvement of the three coupling sites (CI, CIII and CIV) in the catabolic pathway of electrons to O_2. This varies with: (*1*) a bypass of CI by single or multiple electron input into the Q-junction; and (*2*) a bypass of CIV by involvement of AOX. H^+_{pos}/O_2 is 12 in the ET-pathways involving CIII and CIV as proton pumps, increasing to 20 for the NADH-pathway (**Fig. 1A**), but a general consensus on H^+_{pos}/O_2 stoichiometries remains to be reached (Hinkle 2005; Wikström and Hummer 2012; Sazanov 2015). The $H^+_{neg}/\text{P»}$ coupling stoichiometry (3.7; **Fig. 1A**) is the sum of 2.7 H^+_{neg} required by

671   the F-ATPase of vertebrate and most invertebrate species (Watt *et al.* 2010) and the proton
672   balance in the translocation of ADP, ATP and P_i (**Fig. 1B**). Taken together, the mechanistic
673   P»/O_2 ratio is calculated at 5.4 and 3.3 for NADH- and succinate-linked respiration, respectively
674   (Eq. 1). The corresponding classical P»/O ratios (referring to the 2 electron reduction of 0.5 O_2)
675   are 2.7 and 1.6 (Watt *et al.* 2010), in direct agreement with the measured P»/O ratio for succinate
676   of 1.58 ± 0.02 (Gnaiger *et al.* 2000).
677   The effective P»/O_2 flux ratio ($Y_{P»/O_2} = J_{P»}/J_{kO_2}$) is diminished relative to the mechanistic
678   P»/O_2 ratio by intrinsic and extrinsic uncoupling and dyscoupling (**Fig. 3**). Such generalized
679   uncoupling is different from switching to mitochondrial pathways that involve fewer than three
680   proton pumps ('coupling sites': Complexes CI, CIII and CIV), bypassing CI through multiple
681   electron entries into the Q-junction, or CIII and CIV through AOX (**Fig. 1**). Reprogramming of
682   mitochondrial pathways may be considered as a switch of gears (changing the stoichiometry)
683   rather than uncoupling (loosening the stoichiometry). In addition, $Y_{P»/O_2}$ depends on several
684   experimental conditions of flux control, increasing as a hyperbolic function of [ADP] to a
685   maximum value (Gnaiger 2001).
686   The net OXPHOS-capacity is calculated by subtracting *L* from *P* (**Fig. 7**). Then the net
687   P»/O_2 equals P»/(*P-L*), wherein the dissipative LEAK component in the OXPHOS-state may
688   be overestimated. This can be avoided by measuring LEAK-respiration in a state when the
689   protonmotive force is adjusted to its slightly lower value in the OXPHOS-state—by titration of
690   an ET inhibitor (Divakaruni and Brand 2011). Any turnover-dependent components of proton
691   leak and slip, however, are underestimated under these conditions (Garlid *et al.* 1993). In
692   general, it is inappropriate to use the term *ATP production* or *ATP turnover* for the difference
693   of oxygen consumption measured in states *P* and *L*. The difference *P-L* is the upper limit of the
694   part of OXPHOS-capacity that is freely available for ATP production (corrected for LEAK-
695   respiration) and is fully coupled to phosphorylation with a maximum mechanistic stoichiometry
696   (**Fig. 7**).
697   **Control and regulation:** The terms metabolic *control* and *regulation* are frequently used
698   synonymously, but are distinguished in metabolic control analysis: 'We could understand the
699   regulation as the mechanism that occurs when a system maintains some variable constant over
700   time, in spite of fluctuations in external conditions (homeostasis of the internal state). On the
701   other hand, metabolic control is the power to change the state of the metabolism in response to
702   an external signal' (Fell 1997). Respiratory control may be induced by experimental control
703   signals that *exert* an influence on: (*1*) ATP demand and ADP phosphorylation-rate; (*2*) fuel
704   substrate composition, pathway competition; (*3*) available amounts of substrates and oxygen,
705   *e.g.*, starvation and hypoxia; (*3*) the protonmotive force, redox states, flux–force relationships,
706   coupling and efficiency; (*4*) Ca^{2+} and other ions including H^+; (*5*) inhibitors, *e.g.*, nitric oxide
707   or intermediary metabolites such as oxaloacetate; (*6*) signalling pathways and regulatory
708   proteins, *e.g.,* insulin resistance, transcription factor HIF-1 or inhibitory factor 1. *Mechanisms*
709   of respiratory control and regulation include adjustments of: (*1*) enzyme activities by allosteric
710   mechanisms and phosphorylation; (*2*) enzyme content, concentrations of cofactors and
711   conserved moieties—such as adenylates, nicotinamide adenine dinucleotide [NAD^+/NADH],
712   coenzyme Q, cytochrome *c*); (*3*) metabolic channeling by supercomplexes; and *(4)*
713   mitochondrial density (enzyme concentrations and membrane area) and morphology (cristae
714   folding, fission and fusion). (*5*) Mitochondria are targeted directly by hormones, thereby
715   affecting their energy metabolism (Lee *et al.* 2013; Gerö and Szabo 2016; Price and Dai 2016;
716   Moreno *et al.* 2017). Evolutionary or acquired differences in the genetic and epigenetic basis
717   of mitochondrial function (or dysfunction) between subjects and gene therapy; age; gender,
718   biological sex, and hormone concentrations; life style including exercise and nutrition; and
719   environmental issues including thermal, atmospheric, toxicological and pharmacological
720   factors, exert an influence on all control mechanisms listed above. For reviews, see Brown
721   1992; Gnaiger 1993a, 2009; 2014; Paradies *et al.* 2014; Morrow *et al.* 2017.

722   **Respiratory control and response:** Lack of control by a metabolic pathway, *e.g.,*
723 phosphorylation-pathway, does mean that there will be no response to a variable activating it,
724 *e.g.,* [ADP]. The reverse, however, is not true as the absence of a response to [ADP] does not
725 exclude the phosphorylation-pathway from having some degree of control. The degree of
726 control of a component of the OXPHOS-pathway on an output variable—such as oxygen flux,
727 will in general be different from the degree of control on other outputs—such as
728 phosphorylation-flux or proton leak flux. Therefore, it is necessary to be specific as to which
729 input and output are under consideration (Fell 1997).

730   **Respiratory coupling control:** Respiratory control refers to the ability of mitochondria
731 to adjust oxygen consumption in response to external control signals by engaging various
732 mechanisms of control and regulation. Respiratory control is monitored in a mitochondrial
733 preparation under conditions defined as respiratory states. When phosphorylation of ADP to
734 ATP is stimulated or depressed, an increase or decrease is observed in electron flux linked to
735 oxygen consumption in respiratory coupling states of intact mitochondria ('controlled states' in
736 the classical terminology of bioenergetics). Alternatively, coupling of electron transfer with
737 phosphorylation is disengaged by disruption of the integrity of the mtIM or by uncouplers,
738 functioning like a clutch in a mechanical system. The corresponding coupling control state is
739 characterized by high levels of oxygen consumption without control by phosphorylation
740 ('uncontrolled state').

741   **ET-pathway control states** are obtained in mitochondrial preparations by depletion of
742 endogenous substrates and addition to the mitochondrial respiration medium of fuel substrates
743 (CHNO; 2[H]) and specific inhibitors, activating selected mitochondrial catabolic pathways, k
744 (**Fig. 1 and 2**). Coupling control states and pathway control states are complementary, since
745 mitochondrial preparations depend on an exogenous supply of pathway-specific fuel substrates
746 and oxygen (Gnaiger 2014).

747

748 *2.3. Classical terminology for isolated mitochondria*
749   *'When a code is familiar enough, it ceases appearing like a code; one forgets that there*
750   *is a decoding mechanism. The message is identical with its meaning'* (Hofstadter 1979).

751

752 Chance and Williams (1955; 1956) introduced five classical states of mitochondrial respiration
753 and cytochrome redox states. **Table 3** shows a protocol with isolated mitochondria in a closed
754 respirometric chamber, defining a sequence of respiratory states. States and rates are not
755 specifically distinguished in this nomenclature.

756

757   **Table 3. Metabolic states of mitochondria (Chance and**
758   **Williams, 1956; Table V).**
759

State	[O_2]	ADP level	Substrate Level	Respiration rate	Rate-limiting substance
1	>0	low	low	slow	ADP
2	>0	high	~0	slow	substrate
3	>0	high	high	fast	respiratory chain
4	>0	low	high	slow	ADP
5	0	high	high	0	oxygen

760

761

762   **State 1** is obtained after addition of isolated mitochondria to air-saturated
763 isoosmotic/isotonic respiration medium containing inorganic phosphate, but no fuel substrates
764 and no adenylates, *i.e.*, AMP, ADP, ATP.

765   **State 2** is induced by addition of a 'high' concentration of ADP (typically 100 to 300
766 μM), which stimulates respiration transiently on the basis of endogenous fuel substrates and
767 phosphorylates only a small portion of the added ADP. State 2 is then obtained at a low
768 respiratory activity limited by exhausted endogenous fuel substrate availability (**Table 3**). If
769 addition of specific inhibitors of respiratory complexes—such as rotenone—does not cause a
770 further decline of oxygen consumption, State 2 is equivalent to the state of residual oxygen
771 consumption, ROX (See below.). If inhibition is observed, undefined endogenous fuel
772 substrates are a confounding factor of pathway control, contributing to the effect of
773 subsequently externally added substrates and inhibitors. In contrast to the original protocol, an
774 alternative sequence of titration steps is frequently applied, in which the alternative 'State 2'
775 has an entirely different meaning, when this second state is induced by addition of fuel substrate
776 without ADP (LEAK-state; in contrast to State 2 defined in **Table 1** as a ROX state), followed
777 by addition of ADP.

778   **State 3** is the state stimulated by addition of fuel substrates while the ADP concentration
779 is still high (**Table 3**) and supports coupled energy transformation through oxidative
780 phosphorylation. 'High ADP' is a concentration of ADP specifically selected to allow the
781 measurement of State 3 to State 4 transitions of isolated mitochondria in a closed respirometric
782 chamber. Repeated ADP titration re-establishes State 3 at 'high ADP'. Starting at oxygen
783 concentrations near air-saturation (ca. 200 μM O_2 at sea level and 37 °C), the total ADP
784 concentration added must be low enough (typically 100 to 300 μM) to allow phosphorylation
785 to ATP at a coupled rate of oxygen consumption that does not lead to oxygen depletion during
786 the transition to State 4. In contrast, kinetically-saturating ADP concentrations usually are 10-
787 fold higher than 'high ADP', *e.g.,* 2.5 mM in isolated mitochondria. The abbreviation State 3u
788 is occasionally used in bioenergetics, to indicate the state of respiration after titration of an
789 uncoupler, without sufficient emphasis on the fundamental difference between OXPHOS-
790 capacity (*well-coupled* with an *endogenous* uncoupled component) and ET-capacity
791 (*noncoupled*).

792   **State 4** is a LEAK-state that is obtained only if the mitochondrial preparation is intact
793 and well-coupled. Depletion of ADP by phosphorylation to ATP leads to a decline in the rate
794 of oxygen consumption in the transition from State 3 to State 4. Under these conditions of State
795 4, a maximum protonmotive force and high ATP/ADP ratio are maintained. For calculation of
796 P»/O_2 ratios the gradual decline of $Y_{P»/O_2}$ towards diminishing [ADP] at State 4 must be taken
797 into account (Gnaiger 2001). State 4 respiration, L_T (**Table 1**), reflects intrinsic proton leak and
798 intrinsic ATP hydrolysis activity. Oxygen consumption in State 4 is an overestimation of
799 LEAK-respiration if the contaminating ATP hydrolysis activity recycles some ATP to ADP,
800 $J_{P«}$, which stimulates respiration coupled to phosphorylation, $J_{P»} > 0$. This can be tested by
801 inhibition of the phosphorylation-pathway using oligomycin, ensuring that $J_{P»} = 0$ (State 4o).
802 Alternatively, sequential ADP titrations re-establish State 3, followed by State 3 to State 4
803 transitions while sufficient oxygen is available. Anoxia may be reached, however, before
804 exhaustion of ADP (State 5).

805   **State 5** is the state after exhaustion of oxygen in a closed respirometric chamber.
806 Diffusion of oxygen from the surroundings into the aqueous solution may be a confounding
807 factor preventing complete anoxia (Gnaiger 2001). Chance and Williams (1955) provide an
808 alternative definition of State 5, which gives it the different meaning of ROX versus anoxia:
809 'State 5 may be obtained by antimycin A treatment or by anaerobiosis'.

810   In **Table 3**, only States 3 and 4 (and 'State 2' in the alternative protocol: addition of fuel
811 substrates without ADP; not included in the table) are coupling control states, with the
812 restriction that O_2 flux in State 3 may be limited kinetically by non-saturating ADP
813 concentrations (**Table 1**).

814
815

3. Normalization: fluxes and flows

3.1. Normalization: system or sample

The term *rate* is not sufficiently defined to be useful for a database (**Fig. 8**). The inconsistency of the meanings of rate becomes fully apparent when considering Galileo Galilei's famous principle, that 'bodies of different weight all fall at the same rate (have a constant acceleration)' (Coopersmith 2010).

Fig. 8. Different meanings of *rate* may lead to confusion, if the normalization is not sufficiently specified. Results are frequently expressed as mass-specific *flux*, J_{mX}, per mg protein, dry or wet weight (mass). Cell volume, V_{cell}, may be used for normalization (volume-specific flux, J_{Vcell}), which must be clearly distinguished from flow per cell, I_{Ncell}, or flux, J_V, expressed for methodological reasons per volume of the measurement system. For details see **Table 4**.

Flow per system, I: In a generalization of electrical terms, flow as an extensive quantity (per system) is distinguished from flux as a size-specific quantity (per system size) (**Fig. 8**). Electric current is flow, I_{el} [A ≡ C·s^{-1}] per system (extensive quantity). When dividing this extensive quantity by system size (cross-sectional area of a 'wire'), a size-specific quantity is obtained, which is flux (current density), J_{el} [A·m^{-2} = C·s^{-1}·m^{-2}].

Extensive quantities: An extensive quantity increases proportionally with system size. The magnitude of an extensive quantity is completely additive for non-interacting subsystems—such as mass or flow expressed per defined system. The magnitude of these quantities depends on the extent or size of the system (Cohen *et al.* 2008).

Size-specific quantities: 'The adjective *specific* before the name of an extensive quantity is often used to mean *divided by mass*' (Cohen *et al.* 2008). In this system-paradigm, mass-specific flux is flow divided by mass of the *system* (the total mass of everything within the measuring chamber). A mass-specific quantity is independent of the extent of non-interacting homogenous subsystems. Tissue-specific quantities (related to the *sample* in contrast to the *system*) are of fundamental interest in comparative mitochondrial physiology, where *specific* refers to the *type of the sample* rather than *mass of the system*. The term *specific*, therefore, must be clarified; *sample*-specific, *e.g.*, muscle mass-specific normalization, is distinguished from *system*-specific (mass or volume) quantities (**Fig. 8**).

Box 2: Metabolic fluxes and flows: vectorial and scalar

Fluxes are *vectors*, if they have *spatial* direction in addition to magnitude. A vector flux (surface-density of flow) is expressed per unit cross-sectional area, A [m^2], perpendicular to the direction of flux. *Flows* are defined as extensive quantities of the *system*, as vector or scalar flow, $\boldsymbol{I}$ or I [mol·s^{-1}], respectively, then the corresponding vector and scalar *fluxes* are $\boldsymbol{J} = \boldsymbol{I}·A^{-1}$ [mol·s^{-1}·m^{-2}] and $J = I·V^{-1}$ [mol·s^{-1}·m^{-3}], respectively, expressing flux as an area-specific vector
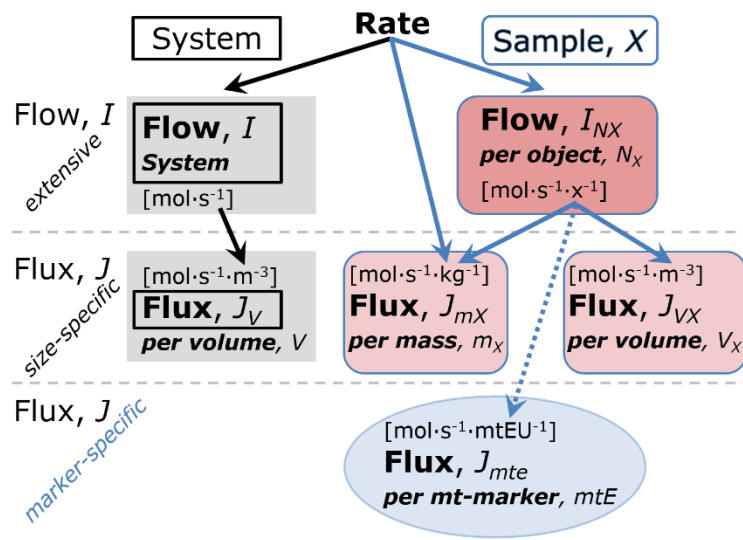
867   or volume-specific scalar quantity. We suggest to define: (*1*) *vectoral* fluxes, which analyze
868   translocations in continuous systems as functions of gradients; (*2*) *vectorial* fluxes, which
869   describe translocations in discontinuous systems and are restricted to information on
870   compartmental differences (**Fig. 2**, transmembrane proton flux); and (*3*) *scalar* fluxes, which
871   are transformations in a homogenous system (**Fig. 2**, catabolic O_2 flux, J_{kO_2} [mol·s^{-1}·m^{-3}]).

872   Vectorial transmembrane proton fluxes, J_{mH+pos} and J_{mH+neg}, are analyzed in a
873   heterogenous compartmental system as a quantity with *directional* but not *spatial* information.
874   Translocation of protons across the mtIM has a defined direction, either from the negative
875   compartment (matrix space; negative, neg–compartment) to the positive compartment (inter-
876   membrane space; positive, pos–compartment) or *vice versa* (**Fig. 2**). The arrows defining the
877   direction of the translocation between the two compartments may point upwards or downwards,
878   right or left, without any implication that these are actual directions in space. The pos–
879   compartment is neither above nor below the neg–compartment in a spatial sense, but can be
880   visualized arbitrarily in a figure in the upper position (**Fig. 2**). In general, the *compartmental*
881   *direction* of vectorial translocation from the neg–compartment to the pos–compartment is
882   defined by assigning the initial and final state as *ergodynamic compartments*, $H^+_{neg} \rightarrow H^+_{pos}$ or
883    $0 = -1\ H^+_{neg} + 1\ H^+_{pos}$, related to work (erg = work) that must be performed to lift the proton from
884   a lower to a higher electrochemical potential or from the lower to the higher ergodynamic
885   compartment (Gnaiger 1993b).

886   In direct analogy to *vectorial* translocation, the direction of a *scalar* chemical reaction, A
887    $\rightarrow$ B or $0 = -1\ A + 1\ B$, is defined by assigning substrates and products, A and B, as ergodynamic
888   compartments. O_2 is defined as a substrate in respiratory O_2 consumption, which together with
889   the fuel substrates comprises the substrate compartment of the catabolic reaction (**Fig. 2**).
890   Volume-specific scalar O_2 flux is coupled to vectorial translocation, yielding the H^+_{pos}/O_2 ratio
891   (**Fig. 1**).

893   *3.2. Normalization for system-size: flux per chamber volume*

895   **System-specific flux, J**: The experimental system (the experimental chamber) is part of
896   the measurement apparatus, separated from the environment as an isolated, closed, open,
897   isothermal or non-isothermal system (**Table 4**). On another level, we distinguish between (*1*)
898   the *system* with volume V and mass m defined by the system boundaries, and (*2*) the *sample* or
899   *objects* with volume V_X and mass m_X which are enclosed in the experimental chamber (**Fig. 8**).
900   Metabolic O_2 flow per object, I_{X,O_2}, increases as the mass of the object is increased. Object mass-
901   specific O_2 flux, J_{mX,O_2} should be independent of the mass of the object studied in the instrument
902   chamber, but system volume-specific O_2 flux, J_{V,O_2} (per volume of the instrument chamber),
903   should increase in direct proportion to the mass of the object in the chamber. J_{V,O_2} depends on
904   mass-concentration of the sample in the chamber, but should be independent of the chamber
905   (system) volume. There are practical limitations to increasing the mass-concentration of the
906   sample in the chamber, when one is concerned about crowding effects and instrumental time
907   resolution.

908   When the reactor volume does not change during the reaction, which is typical for liquid
909   phase reactions, the volume-specific *flux of a chemical reaction* r is the time derivative of the
910   advancement of the reaction per unit volume, $J_{V,rB} = d_r\xi_B/dt \cdot V^{-1}$ [(mol·s^{-1})·L^{-1}]. The *rate of*
911   *concentration change* is dc_B/dt [(mol·L^{-1})·s^{-1}], where concentration is $c_B = n_B/V$. There is a
912   difference between (*1*) J_{V,rO_2} [mol·s^{-1}·L^{-1}] and (*2*) rate of concentration change [mol·L^{-1}·s^{-1}].
913   These merge to a single expression only in closed systems. In open systems, external fluxes
914   (such as O_2 supply) are distinguished from internal transformations (metabolic flux, O_2
915   consumption). In a closed system, external flows of all substances are zero and O_2 consumption
916   (internal flow of catabolic reactions k), I_{kO_2} [pmol·s^{-1}], causes a decline of the amount of O_2 in
917   the system, n_{O_2} [nmol]. Normalization of these quantities for the volume of the system, V [L $\equiv$

918 dm^3], yields volume-specific O$_2$ flux, $J_{V,kO_2} = I_{kO_2}/V$ [nmol·s^{-1}·L^{-1}], and O$_2$ concentration, [O$_2$]
919 or $c_{O_2} = n_{O_2}/V$ [µmol·L^{-1} = µM = nmol·mL^{-1}]. Instrumental background O$_2$ flux is due to external
920 flux into a non-ideal closed respirometer; then total volume-specific flux has to be corrected for
921 instrumental background O$_2$ flux—O$_2$ diffusion into or out of the instrumental chamber. J_{V,kO_2}
922 is relevant mainly for methodological reasons and should be compared with the accuracy of
923 instrumental resolution of background-corrected flux, *e.g.*, ±1 nmol·s^{-1}·L^{-1} (Gnaiger 2001).
924 'Metabolic' or catabolic indicates O$_2$ flux, J_{kO_2}, corrected for: (*1*) instrumental background O$_2$
925 flux; (*2*) chemical background O$_2$ flux due to autoxidation of chemical components added to
926 the incubation medium; and (*3*) *Rox* for O$_2$-consuming side reactions unrelated to the catabolic
927 pathway k.

929 *3.3. Normalization: per sample*

931 The challenges of measuring mitochondrial respiratory flux are matched by those of
932 normalization. Application of common and defined units is required for direct transfer of
933 reported results into a database. The second [s] is the *SI* unit for the base quantity *time*. It is also
934 the standard time-unit used in solution chemical kinetics. A rate may be considered as the
935 numerator and normalization as the complementary denominator, which are tightly linked in
936 reporting the measurements in a format commensurate with the requirements of a database.
937 Normalization (**Table 4**) is guided by physicochemical principles, methodological
938 considerations (**Fig. 9**), and conceptual strategies (**Fig. 10**).

940
941 **Table 4. Sample concentrations and normalization of flux.**

Expression	Symbol	Definition	Unit	Notes
Sample				
identity of sample	X	object: cell, tissue, animal, patient		
number of sample entities X	N_X	number of objects	x	
mass of sample X	m_X		kg	1
mass of object X	M_X	$M_X = m_X·N_X^{-1}$	kg·x^{-1}	1
Mitochondria				
Mitochondria	mt	X = mt		
amount of mt-elements	*mtE*	quantity of mt-marker	mtEU	
Concentrations				
object number concentration	C_{NX}	$C_{NX} = N_X·V^{-1}$	x·m^{-3}	2
sample mass concentration	C_{mX}	$C_{mX} = m_X·V^{-1}$	kg·m^{-3}	
mitochondrial concentration	C_{mtE}	$C_{mtE} = mtE·V^{-1}$	mtEU·m^{-3}	3
specific mitochondrial density	D_{mtE}	$D_{mtE} = mtE·m_X^{-1}$	mtEU·kg^{-1}	4
mitochondrial content, *mtE* per object X	mtE_X	$mtE_X = mtE·N_X^{-1}$	mtEU·x^{-1}	5
O$_2$ flow and flux				6
flow, system	I_{O_2}	internal flow	mol·s^{-1}	7
volume-specific flux	J_{V,O_2}	$J_{V,O_2} = I_{O_2}·V^{-1}$	mol·s^{-1}·m^{-3}	8
flow per object X	I_{X,O_2}	$I_{X,O_2} = J_{V,O_2}·C_{NX}^{-1}$	mol·s^{-1}·x^{-1}	9
mass-specific flux	J_{mX,O_2}	$J_{mX,O_2} = J_{V,O_2}·C_{mX}^{-1}$	mol·s^{-1}·kg^{-1}	
mitochondria-specific flux	J_{mtE,O_2}	$J_{mtE,O_2} = J_{V,O_2}·C_{mtE}^{-1}$	mol·s^{-1}·mtEU^{-1}	10

942   1 The *SI* prefix k is used for the SI base unit of mass (kg = 1,000 g). In praxis, various *SI* prefixes are
943   used for convenience, to make numbers easily readable, *e.g.,* 1 mg tissue, cell or mitochondrial mass
944   instead of 0.000001 kg.
945   2 In case sample X = cells, the object number concentration is $C_{Ncell} = N_{cell} \cdot V^{-1}$, and volume may be
946   expressed in [dm$^3 \equiv$ L] or [cm^3 = mL]. See **Table 5** for different object types.
947   3 mt-concentration is an experimental variable, dependent on sample concentration: (*1*) $C_{mtE} = mtE \cdot V^{-1}$;
948   (*2*) $C_{mtE} = mtE_X \cdot C_{NX}$; (*3*) $C_{mtE} = C_{mX} \cdot D_{mtE}$.
949   4 If the amount of mitochondria, mtE, is expressed as mitochondrial mass, then D_{mtE} is the mass
950   fraction of mitochondria in the sample. If mtE is expressed as mitochondrial volume, V_{mt}, and the
951   mass of sample, m_X, is replaced by volume of sample, V_X, then D_{mtE} is the volume fraction of
952   mitochondria in the sample.
953   5 $mtE_X = mtE \cdot N_X^{-1} = C_{mtE} \cdot C_{NX}^{-1}$.
954   6 O_2 can be replaced by other chemicals B to study different reactions, *e.g.,* ATP, H_2O_2, or
955   compartmental translocations, *e.g.,* Ca^{2+}.
956   7 I_{O_2} and V are defined per instrument chamber as a system of constant volume (and constant
957   temperature), which may be closed or open. I_{O_2} is abbreviated for I_{O_2r}—the metabolic or internal O_2
958   flow of the chemical reaction r in which O_2 is consumed—hence the negative stoichiometric number,
959   v_{O_2} = -1. $I_{O_2r} = d_r n_{O_2}/dt \cdot v_{O_2}^{-1}$. If r includes all chemical reactions in which O_2 participates, then $d_r n_{O_2} = dn_{O_2}$
960       $- d_e n_{O_2}$, where dn_{O_2} is the change in the amount of O_2 in the instrument chamber and $d_e n_{O_2}$ is the
961   amount of O_2 added externally to the system. At steady state, by definition $dn_{O_2} = 0$, hence $d_r n_{O_2} = -$
962       $d_e n_{O_2}$.
963   8 J_{V,O_2} is an experimental variable, expressed per volume of the instrument chamber.
964   9 I_{X,O_2} is a physiological variable, depending on the size of entity X.
965 10 There are many ways to normalize for a mitochondrial marker, that are used in different experimental
966   approaches: (*1*) $J_{mtE,O_2} = J_{V,O_2} \cdot C_{mtE}^{-1}$; (*2*) $J_{mtE,O_2} = J_{V,O_2} \cdot C_{mX}^{-1} \cdot D_{mtE}^{-1} = J_{mX,O_2} \cdot D_{mtE}^{-1}$; (*3*) $J_{mtE,O_2} =$
967       $J_{V,O_2} \cdot C_{NX}^{-1} \cdot mtE_X^{-1} = I_{X,O_2} \cdot mtE_X^{-1}$; (*4*) $J_{mtE,O_2} = I_{O_2} \cdot mtE^{-1}$. The mt-elemental unit [mtEU] varies between
968   different mt-markers.
969
970   **Table 5. Sample types, *X*, abbreviations, and quantification.**

Identity of sample	X	N_X	Mass[a]	Volume	mt-Marker
mitochondrial preparation	mtprep	[x]	[kg]	[m^3]	[mtEU]
isolated mitochondria	imt		m_{mt}	V_{mt}	mtE
tissue homogenate	thom		m_{thom}		mtE_{thom}
permeabilized tissue	pti		m_{pti}		mtE_{pti}
permeabilized fibre	pfi		m_{pfi}		mtE_{pfi}
permeabilized cell	pce	N_{pce}	M_{pce}	V_{pce}	mtE_{pce}
intact cell	ce	N_{ce}	M_{ce}	V_{ce}	mtE_{ce}
Organism	org	N_{org}	M_{org}	V_{org}	

971   [a] Instead of mass, frequently the wet weight or dry weight is stated, W_w or W_d.
972   m_X is mass of the sample [kg], M_X is mass of the object [kg·x^{-1}].
973

974   **Sample concentration, C_{mX}:** Normalization for sample concentration is required for
975 reporting respiratory data. Consider a tissue or cells as the sample, X, and the sample mass, m_X
976 [mg] from which a mitochondrial preparation is obtained. m_X is frequently measured as wet or
977 dry weight, W_w or W_d [mg], or as amount of tissue or cell protein, $m_{Protein}$. In the case of
978 permeabilized tissues, cells, and homogenates, the sample concentration, $C_{mX} = m_X/V$ [mg·mL^{-1}
979 = g·L^{-1}], is simply the mass of the subsample of tissue that is transferred into the instrument
980 chamber.
981   **Mass-specific flux, J_{mX,O_2}:** Mass-specific flux is obtained by expressing respiration per
982 mass of sample, m_X [mg]. X is the type of sample—tissue homogenate, permeabilized fibres or
983 cells. Volume-specific flux is divided by mass concentration of X, $J_{mX,O_2} = J_{V,O_2}/C_{mX}$; or flow
984 per cell is divided by mass per cell, $J_{mcell,O_2} = I_{cell,O_2}/M_{cell}$. If mass-specific O_2 flux is constant
985 and independent of sample size (expressed as mass), then there is no interaction between the
986 subsystems. A 1.5 mg and a 3.0 mg muscle sample respires at identical mass-specific flux.
987 Mass-specific O_2 flux, however, may change with the mass of a tissue sample, cells or isolated

988 mitochondria in the measuring chamber, in which case the nature of the interaction becomes an
989 issue. Therefore, cell density must be optimization, particularly in experiments carried out in
990 wells, considering the confluency of the cell monolayer or clumps of cells (Salabei *et al.* 2014).
991 **Number concentration, C_{NX}:** C_{NX} is the experimental *number concentration* of sample
992 *X*. In the case of cells or animals, *e.g.*, nematodes, $C_{NX} = N_X/V$ [x·L^{-1}], where N_X is the number
993 of cells or organisms in the chamber (**Table 4**).
994 **Flow per object, I_{X,O_2}:** A special case of normalization is encountered in respiratory
995 studies with permeabilized (or intact) cells. If respiration is expressed per cell, the O$_2$ flow per
996 measurement system is replaced by the O$_2$ flow per cell, I_{cell,O_2} (**Table 4**). O$_2$ flow can be
997 calculated from volume-specific O$_2$ flux, J_{V,O_2} [nmol·s^{-1}·L^{-1}] (per *V* of the measurement chamber
998 [L]), divided by the number concentration of cells, $C_{Nce} = N_{ce}/V$ [cell·L^{-1}], where N_{ce} is the
999 number of cells in the chamber. Cellular O$_2$ flow can be compared between cells of identical
1000 size. To take into account changes and differences in cell size, normalization is required to
1001 obtain cell size-specific or mitochondrial marker-specific O$_2$ flux (Renner *et al.* 2003).
1002 The complexity changes when the sample is a whole organism studied as an experimental
1003 model. The scaling law in respiratory physiology reveals a strong interaction of O$_2$ consumption
1004 and individual body mass of an organism, since *basal* metabolic rate (flow) does not increase
1005 linearly with body mass, whereas *maximum* mass-specific O$_2$ flux, $\dot{V}_{O2max}$ or $\dot{V}_{O2peak}$, is
1006 approximately constant across a large range of individual body mass (Weibel and Hoppeler
1007 2005), with individuals, breeds, and species deviating substantially from this relationship.
1008 $\dot{V}_{O2peak}$ of human endurance athletes is 60 to 80 mL O$_2$·min^{-1}·kg^{-1} body mass, converted to
1009 $J_{M,O2peak}$ of 45 to 60 nmol·s^{-1}·g^{-1} (Gnaiger 2014; **Table 6**).

1011 *3.4. Normalization for mitochondrial content*

1013 Tissues can contain multiple cell populations which may have distinct mitochondrial
1014 subtypes. Mitochondria undergo dynamic fission and fusion cycles, and can exist in multiple
1015 stages and sizes which may be altered by a range of factors. The isolation of mitochondria (often
1016 achieved through differential centrifugation) can therefore yield a subsample of the
1017 mitochondrial types present in a tissue, dependent on isolation protocols utilized (*e.g.,*
1018 centrifugation speed). This possible artefact should be taken into account when planning
1019 experiments using isolated mitochondria. Different sizes of mitochondria are enriched at
1020 specific centrifugation speeds, which is used for isolation of mitochondrial subpopulations.
1021 Part of the mitochondrial content of a tissue is lost during preparation of isolated
1022 mitochondria. The fraction of mitochondria in the isolate is expressed as mitochondrial
1023 recovery (**Fig. 9**). At a high mitochondrial recovery the sample of isolated mitochondria is more
1024 representative of the total mitochondrial population than in preparations characterized by low
1025 recovery. Determination of the mitochondrial recovery and yield is based on measurement of
1026 the concentration of a mitochondrial marker in the tissue homogenate, $C_{mtE,thom}$, which
1027 simultaneously provides information on the specific mitochondrial density in the sample (**Fig.
1028 9**).
1029 Normalization is a problematic subject; it is essential to consider the question of the study.
1030 If the study aims at comparing tissue performance—such as the effects of a treatment on a
1031 specific tissue, then normalization can be successful, using tissue mass or protein content, for
1032 example. If the aim, however, is to find differences of mitochondrial function independent of
1033 mitochondrial density (**Table 4**), then normalization to a mitochondrial marker is imperative
1034 (**Fig. 10**). One cannot assume that quantitative changes in various markers—such as
1035 mitochondrial proteins—necessarily occur in parallel with one another. It should be established
1036 that the marker chosen is not selectively altered by the performed treatment. In conclusion, the
1037 normalization must reflect the question under investigation to reach a satisfying answer. On the

1038 other hand, the goal of comparing results across projects and institutions requires
1039 standardization on normalization for entry into a databank.
1040
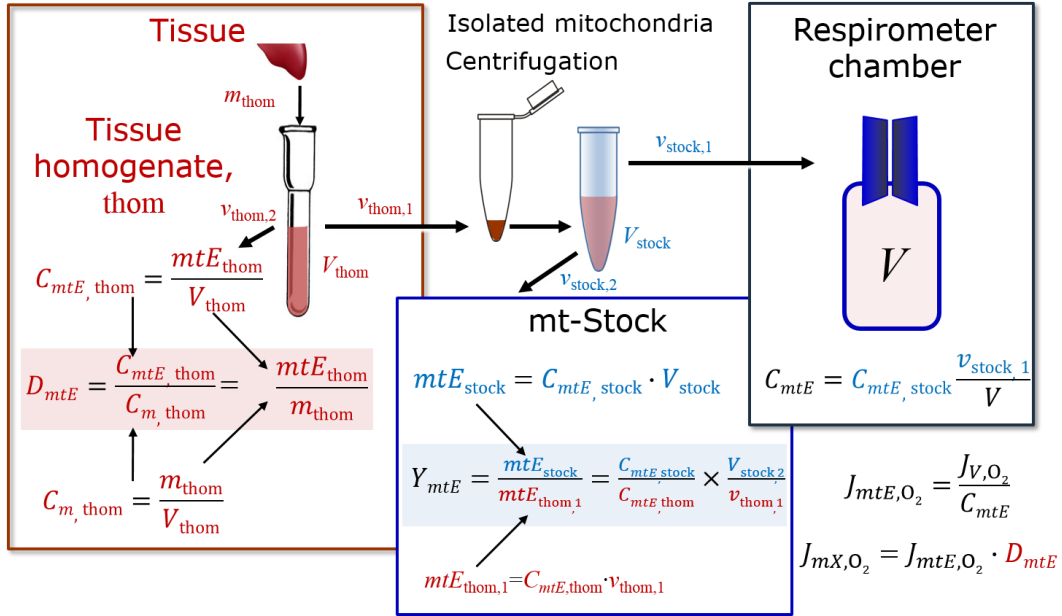
1041
1042

Symbol	Definition [Units]
C_{mtE}	mitochondrial concentration in chamber [mtEU·L^{-1}]
C_m	sample mass concentration in chamber [g·L^{-1}]
D_{mtE}	specific mte-density per tissue mass [mtEU·g^{-1}]
J_{m,O_2}	mass-specific O$_2$ flux [nmol·s^{-1}·g^{-1}]
J_{mtE,O_2}	mitochondria-specific O$_2$ flux [nmol·s^{-1}·mtEU^{-1}]
mtE	amount of mitochondrial elements [mtEU]
m_{thom}	mass of tissue in the homogenate [g]
Y_{mtE}	recovery of isolated mitochondria
$Y_{mtE/m}$	yield of isolated mitochondria; $Y_{mtE/m} = Y_{mtE} \cdot D_{mtE}$ [mtEU·g^{-1}]
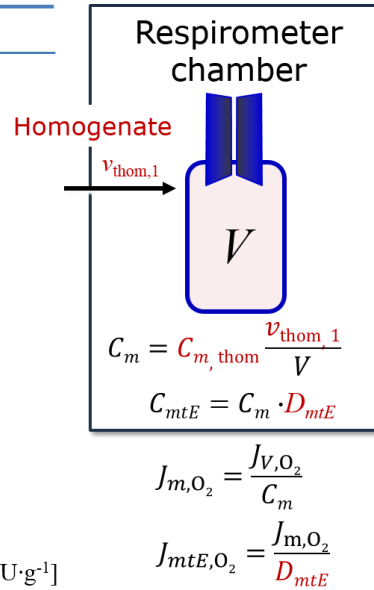
1043
1044 **Fig. 9. Normalization of volume-specific flux of isolated mitochondria and tissue**
1045 **homogenate. A:** Recovery, Y_{mtE}, in preparation of isolated mitochondria. $v_{thom,1}$ and $v_{stock,1}$ are
1046 the volumes transferred from the total volume, V_{thom} and V_{stock}, respectively. $mtE_{thom,1}$ is the
1047 amount of mitochondrial elements in volume $v_{thom,1}$ used for isolation. **B:** Homogenate, $v_{thom,1}$
1048 is transferred directly into the respirometer chamber. See **Table 4** for further symbols.
1049
1050 **Mitochondrial concentration, C_{mtE}, and mitochondrial markers:** Mitochondrial
1051 concentration in the tissue and the measurement chamber are quantified as (*1*) a physiological
1052 output that is the result of mitochondrial biogenesis and degradation, and (*2*) a quantity for
1053 normalization in functional analyses. Mitochondrial organelles comprise a dynamic cellular
1054 reticulum in various states of fusion and fission. Hence the definition of an "amount" of
1055 mitochondria is often misconceived: mitochondria cannot be counted reliably as a number of
1056 occurring elements. Therefore, quantification of the "amount" of mitochondria depends on
1057 measurement of chosen mitochondrial markers. 'Mitochondria are the structural and functional
1058 elemental units of cell respiration' (Gnaiger 2014). The quantity of a mitochondrial marker can

1059 be considered to reflect the amount of *mitochondrial elements*, *mtE*, expressed in various
1060 mitochondrial elemental units [mtEU] specific for each measured mt-marker (**Table 4**).
1061 However, since mitochondrial quality may change in response to stimuli—particularly in
1062 mitochondrial dysfunction and after exercise training (Pesta *et al.* 2011; Campos *et al.* 2017)—
1063 some markers can vary while others are unchanged: (*1*) Mitochondrial volume and membrane
1064 area are structural markers, whereas mitochondrial protein mass is frequently used as a marker
1065 for isolated mitochondria. (*2*) Molecular and enzymatic mitochondrial markers (amounts or
1066 activities) can be selected as matrix markers, *e.g.*, citrate synthase activity, mtDNA; mtIM-
1067 markers, *e.g.*, cytochrome *c* oxidase activity, *aa₃* content, cardiolipin, or mtOM-markers, *e.g.*,
1068 TOM20. (*3*) Extending the measurement of mitochondrial marker enzyme activity to
1069 mitochondrial pathway capacity, ET- or OXPHOS-capacity can be considered as an integrative
1070 functional mitochondrial marker.
1071

1072
1073 **Fig. 10. Structure-function analysis of performance of an organism, organ or tissue, or a**
1074 **cell (sample entity, *X*). O₂ flow, I_{X,O_2}, is the product of performance per functional element**
1075 **(element function, mitochondria-specific flux), element density (mitochondrial density,**
1076 **D_{mtE}), and size of entity *X* (mass, M_X). (A)** Structured analysis: performance is the product of
1077 mitochondrial *function* (mt-specific flux) and *structure* (functional elements; D_{mtE} times mass
1078 of *X*). (**B**) Unstructured analysis: performance is the product of *entity mass-specific flux*, J_{mX,O_2}
1079 $= I_{X,O_2}/M_X = I_{O_2}/m_X$ [mol·s⁻¹·kg⁻¹] and *size of entity*, expressed as mass of *X*; $M_X = m_X·N_X^{-1}$
1080 [kg·x⁻¹]. See **Table 4** for further explanation of quantities and units. Modified from Gnaiger
1081 (2014).
1082

1083   Depending on the type of mitochondrial marker, the mitochondrial elements, *mtE*, are
1084 expressed in marker-specific units. It is recommended to distinguish *experimental*
1085 *mitochondrial concentration*, $C_{mtE} = mtE/V$ and *physiological mitochondrial density*, $D_{mtE} =$
1086 mtE/m_X. Then mitochondrial density is the amount of mitochondrial elements per mass of tissue,
1087 which is a biological varible (**Fig. 10**). The experimental variable is mitochondrial density
1088 multiplied by sample mass concentration in the measuring chamber, $C_{mtE} = D_{mtE}·C_{mX}$, or
1089 mitochondrial content multiplied by sample number concentration, $C_{mtE} = mtE_X·C_{NX}$ (**Table 4**).
1090   **Mitochondria-specific flux, J_{mtE,O_2}:** Volume-specific metabolic O₂ flux depends on: (*1*)
1091 the sample concentration in the volume of the instrument chamber, C_{mX}, or C_{NX}; (*2*) the

1092   mitochondrial density in the sample, $D_{mtE} = mtE/m_X$ or $mtE_X = mtE/N_X$; and (*3*) the specific
1093   mitochondrial activity or performance per elemental mitochondrial unit, $J_{mtE,O_2} = J_{V,O_2}/C_{mtE}$
1094   [mol·s^{-1}·mtEU^{-1}] (**Table 4**). Obviously, the numerical results for J_{mtE,O_2} vary with the type of
1095   mitochondrial marker chosen for measurement of *mtE* and $C_{mtE} = mtE/V$ [mtEU·m^{-3}].

1096
1097   *3.5. Evaluation of mitochondrial markers*
1098
1099   Different methods are implicated in quantification of mitochondrial markers and have
1100   different strengths. Some problems are common for all mitochondrial markers, *mtE*: (*1*)
1101   Accuracy of measurement is crucial, since even a highly accurate and reproducible
1102   measurement of O_2 flux results in an inaccurate and noisy expression normalized for a biased
1103   and noisy measurement of a mitochondrial marker. This problem is acute in mitochondrial
1104   respiration because the denominators used (the mitochondrial markers) are often small moieties
1105   whose accurate and precise determination is difficult. This problem can be avoided when O_2
1106   fluxes measured in substrate-uncoupler-inhibitor titration protocols are normalized for flux in
1107   a defined respiratory reference state, which is used as an *internal* marker and yields flux control
1108   ratios, *FCR*s (**Fig. 8**). *FCR*s are independent of any *externally* measured markers and, therefore,
1109   are statistically robust, considering the limitations of ratios in general (Jasienski and Bazzaz
1110   1999). *FCR*s indicate qualitative changes of mitochondrial respiratory control, with highest
1111   quantitative resolution, separating the effect of mitochondrial density or concentration on J_{mX,O_2}
1112   and I_{X,O_2} from that of function per elemental mitochondrial marker, J_{mtE,O_2} (Pesta *et al.* 2011;
1113   Gnaiger 2014). (*2*) If mitochondrial quality does not change and only the amount of
1114   mitochondria varies as a determinant of mass-specific flux, any marker is equally qualified in
1115   principle; then in practice selection of the optimum marker depends only on the accuracy and
1116   precision of measurement of the mitochondrial marker. (*3*) If mitochondrial flux control ratios
1117   change, then there may not be any best mitochondrial marker. In general, measurement of
1118   multiple mitochondrial markers enables a comparison and evaluation of normalization for a
1119   variety of mitochondrial markers. Particularly during postnatal development, the activity of
1120   marker enzymes—such as cytochrome *c* oxidase and citrate synthase—follows different time
1121   courses (Drahota *et al.* 2004). Evaluation of mitochondrial markers in healthy controls is
1122   insufficient for providing guidelines for application in the diagnosis of pathological states and
1123   specific treatments.
1124   In line with the concept of the respiratory control ratio (Chance and Williams 1955a), the
1125   most readily used normalization is that of flux control ratios and flux control factors (Gnaiger
1126   2014). Selection of the state of maximum flux in a protocol as the reference state has the
1127   advantages of: (*1*) internal normalization; (*2*) statistical linearization of the response in the range
1128   of 0 to 1; and (*3*) consideration of maximum flux for integrating a large number of elemental
1129   steps in the OXPHOS- or ET-pathways. This reduces the risk of selecting a functional marker
1130   that is specifically altered by the treatment or pathology, yet increases the chance that the
1131   highly integrative pathway is disproportionately affected, *e.g.,* the OXPHOS- rather than ET-
1132   pathway in case of an enzymatic defect in the phosphorylation-pathway. In this case, additional
1133   information can be obtained by reporting flux control ratios based on a reference state which
1134   indicates stable tissue-mass specific flux. Stereological determination of mitochondrial content
1135   via two-dimensional transmission electron microscopy can have limitations due to the dynamics
1136   of mitochondrial size (Meinild Lundby *et al.* 2017). Accurate determination of three-
1137   dimensional volume by two-dimensional microscopy can be both time consuming and
1138   statistically challenging (Larsen *et al.* 2012).
1139   The validity of using mitochondrial marker enzymes (citrate synthase activity, Complex
1140   I–IV amount or activity) for normalization of flux is limited in part by the same factors that
1141   apply to flux control ratios. Strong correlations between various mitochondrial markers and
1142   citrate synthase activity (Reichmann *et al.* 1985; Boushel *et al.* 2007; Mogensen *et al.* 2007)

1143 are expected in a specific tissue of healthy subjects and in disease states not specifically
1144 targeting citrate synthase. Citrate synthase activity is acutely modifiable by exercise
1145 (Tonkonogi *et al.* 1997; Leek *et al.* 2001). Evaluation of mitochondrial markers related to a
1146 selected age and sex cohort cannot be extrapolated to provide recommendations for
1147 normalization in respirometric diagnosis of disease, in different states of development and
1148 ageing, different cell types, tissues, and species. mtDNA normalised to nDNA via qPCR is
1149 correlated to functional mitochondrial markers including OXPHOS- and ET-capacity in some
1150 cases (Puntschart *et al.* 1995; Wang *et al.* 1999; Menshikova *et al.* 2006; Boushel *et al.* 2007),
1151 but lack of such correlations have been reported (Menshikova *et al.* 2005; Schultz and Wiesner
1152 2000; Pesta *et al.* 2011). Several studies indicate a strong correlation between cardiolipin
1153 content and increase in mitochondrial function with exercise (Menshikova *et al.* 2005;
1154 Menshikova *et al.* 2007; Larsen *et al.* 2012; Faber *et al.* 2014), but its use as a general
1155 mitochondrial biomarker in disease remains questionable.

1156
1157 *3.6. Conversion: units*
1158
1159 Many different units have been used to report the rate of oxygen consumption, OCR
1160 (**Table 6**). *SI* base units provide the common reference for introducing the theoretical principles
1161 (**Fig. 8**), and are used with appropriately chosen *SI* prefixes to express numerical data in the
1162 most practical format, with an effort towards unification within specific areas of application
1163 (**Table 7**). Reporting data in *SI* units—including the mole [mol], coulomb [C], joule [J], and
1164 second [s]—should be encouraged, particularly by journals which propose the use of *SI* units.
1165 Although volume is expressed as m^3 using the *SI* base unit, the litre [dm^3] is a
1166 conventional unit of volume for concentration and is used for most solution chemical kinetics.
1167 If one multiplies I_{cell,O_2} by C_{Ncell}, then the result will not only be the amount of O_2 [mol]
1168 consumed per time [s^{-1}] in one litre [L^{-1}], but also the change in the concentration of oxygen per
1169 second (for any volume of an ideally closed system). This is ideal for kinetic modeling as it
1170 blends with chemical rate equations where concentrations are typically expressed in $mol·L^{-1}$
1171 (Wagner *et al.* 2011). In studies of multinuclear cells—such as differentiated skeletal muscle
1172 cells—it is easy to determine the number of nuclei but not the total number of cells. A
1173 generalized concept, therefore, is obtained by substituting cells by nuclei as the sample entity.
1174 This does not hold, however, for enucleated platelets.
1175 For studies of cells, we recommend that respiration be expressed, as far as possible, as:
1176 (*1*) O_2 flux normalized for a mitochondrial marker, for separation of the effects of mitochondrial
1177 quality and content on cell respiration (this includes *FCR*s as a normalization for a functional
1178 mitochondrial marker); (*2*) O_2 flux in units of cell volume or mass, for comparison of respiration
1179 of cells with different cell size (Renner *et al.* 2003) and with studies on tissue preparations, and
1180 (*3*) O_2 flow in units of attomole (10^{-18} mol) of O_2 consumed in a second by each cell
1181 [$amol·s^{-1}·cell^{-1}$], numerically equivalent to [$pmol·s^{-1}·10^{-6}$ cells]. This convention allows
1182 information to be easily used when designing experiments in which oxygen consumption must
1183 be considered. For example, to estimate the volume-specific O_2 flux in an instrument chamber
1184 that would be expected at a particular cell number concentration, one simply needs to multiply
1185 the flow per cell by the number of cells per volume of interest. This provides the amount of O_2
1186 [mol] consumed per time [s^{-1}] per unit volume [L^{-1}]. At an O_2 flow of 100 $amol·s^{-1}·cell^{-1}$ and a
1187 cell density of 10^9 $cells·L^{-1}$ (10^6 $cells·mL^{-1}$), the volume-specific O_2 flux is 100 $nmol·s^{-1}·L^{-1}$ (100
1188 $pmol·s^{-1}·mL^{-1}$).
1189
1190
1191
1192

Table 6. Conversion of various units used in respirometry and ergometry. e^- is the number of electrons or reducing equivalents. z_B is the charge number of entity B.

1 Unit		x	Multiplication factor	SI-unit	Note
ng.atom O·s^{-1}	(2 e$^-$)		0.5	nmol O$_2$·s^{-1}	
ng.atom O·min^{-1}	(2 e$^-$)		8.33	pmol O$_2$·s^{-1}	
natom O·min^{-1}	(2 e$^-$)		8.33	pmol O$_2$·s^{-1}	
nmol O$_2$·min^{-1}	(4 e$^-$)		16.67	pmol O$_2$·s^{-1}	
nmol O$_2$·h^{-1}	(4 e$^-$)		0.2778	pmol O$_2$·s^{-1}	
mL O$_2$·min^{-1} at STPD^a			0.744	μmol O$_2$·s^{-1}	1
W = J/s at -470 kJ/mol O$_2$			-2.128	μmol O$_2$·s^{-1}	
mA = mC·s^{-1}	(z_{H+} = 1)		10.36	nmol H$^+$·s^{-1}	2
mA = mC·s^{-1}	(z_{O_2} = 4)		2.59	nmol O$_2$·s^{-1}	2
nmol H$^+$·s^{-1}	(z_{H+} = 1)		0.09649	mA	3
nmol O$_2$·s^{-1}	(z_{O_2} = 4)		0.38594	mA	3

1 At standard temperature and pressure dry (STPD: 0 °C = 273.15 K and 1 atm = 101.325 kPa = 760 mmHg), the molar volume of an ideal gas, V_m, and V_{m,O_2} is 22.414 and 22.392 L·mol^{-1}, respectively. Rounded to three decimal places, both values yield the conversion factor of 0.744. For comparison at NTPD (20 °C), V_{m,O_2} is 24.038 L·mol^{-1}. Note that the SI standard pressure is 100 kPa.
2 The multiplication factor is $10^6/(z_B·F)$.
3 The multiplication factor is $z_B·F/10^6$.

Table 7. Conversion of units with preservation of numerical values.

Name		Frequently used unit	Equivalent unit	Note
volume-specific flux, J_{V,O_2}		pmol·s^{-1}·mL^{-1}	nmol·s^{-1}·L^{-1}	1
		mmol·s^{-1}·L^{-1}	mol·s^{-1}·m^{-3}	
cell-specific flow, I_{O_2}		pmol·s^{-1}·10^{-6} cells	amol·s^{-1}·cell^{-1}	2
		pmol·s^{-1}·10^{-9} cells	zmol·s^{-1}·cell^{-1}	3
cell number concentration, C_{Nce}		10^6 cells·mL^{-1}	10^9 cells·L^{-1}	
mitochondrial protein concentration, C_{mtE}		0.1 mg·mL^{-1}	0.1 g·L^{-1}	
mass-specific flux, J_{m,O_2}		pmol·s^{-1}·mg^{-1}	nmol·s^{-1}·g^{-1}	4
catabolic power, P_k		μW·10^{-6} cells	pW·cell^{-1}	1
Volume		1,000 L	m^3 (1,000 kg)	
		L	dm^3 (kg)	
		mL	cm^3 (g)	
		μL	mm^3 (mg)	
		fL	μm^3 (pg)	5
amount of substance concentration		M = mol·L^{-1}	mol·dm^{-3}	

1 pmol: picomole = 10^{-12} mol
2 amol: attomole = 10^{-18} mol
3 zmol: zeptomole = 10^{-21} mol
4 nmol: nanomole = 10^{-9} mol
5 fL: femtolitre = 10^{-15} L

1212   ET-capacity in human cell types including HEK 293, primary HUVEC and fibroblasts
1213 ranges from 50 to 180 amol·s^{-1}·cell^{-1}, measured in intact cells in the noncoupled state (see
1214 Gnaiger 2014). At 100 amol·s^{-1}·cell^{-1} corrected for *Rox*, the current across the mt-membranes,
1215 I_{eH+}, approximates 193 pA·cell^{-1} or 0.2 nA per cell. See Rich (2003) for an extension of
1216 quantitative bioenergetics from the molecular to the human scale, with a transmembrane proton
1217 flux equivalent to 520 A in an adult at a catabolic power of -110 W. Modelling approaches
1218 illustrate the link between protonmotive force and currents (Willis *et al.* 2016).

1219   We consider isolated mitochondria as powerhouses and proton pumps as molecular
1220 machines to relate experimental results to energy metabolism of the intact cell. The cellular
1221 P»/O$_2$ based on oxidation of glycogen is increased by the glycolytic (fermentative) substrate-
1222 level phosphorylation of 3 P»/Glyc or 0.5 mol P» for each mol O$_2$ consumed in the complete
1223 oxidation of a mol glycosyl unit (Glyc). Adding 0.5 to the mitochondrial P»/O$_2$ ratio of 5.4
1224 yields a bioenergetic cell physiological P»/O$_2$ ratio close to 6. Two NADH equivalents are
1225 formed during glycolysis and transported from the cytosol into the mitochondrial matrix, either
1226 by the malate-aspartate shuttle or by the glycerophosphate shuttle resulting in different
1227 theoretical yields of ATP generated by mitochondria, the energetic cost of which potentially
1228 must be taken into account. Considering also substrate-level phosphorylation in the TCA cycle,
1229 this high P»/O$_2$ ratio not only reflects proton translocation and OXPHOS studied in isolation,
1230 but integrates mitochondrial physiology with energy transformation in the living cell (Gnaiger
1231 1993a).

1232
1233

1234 **4. Conclusions**

1235

1236   MitoEAGLE can serve as a gateway to better diagnose mitochondrial respiratory defects
1237 linked to genetic variation, age-related health risks, sex-specific mitochondrial performance,
1238 lifestyle with its effects on degenerative diseases, and thermal and chemical environment. The
1239 present recommendations on coupling control states and rates, linked to the concept of the
1240 protonmotive force, are focused on studies with mitochondrial preparations. These will be
1241 extended in a series of reports on pathway control of mitochondrial respiration, respiratory
1242 states in intact cells, and harmonization of experimental procedures.

1243   The optimal choice for expressing mitochondrial and cell respiration (**Box 3**) as O$_2$ flow
1244 per biological system, and normalization for specific tissue-markers (volume, mass, protein)
1245 and mitochondrial markers (volume, protein, content, mtDNA, activity of marker enzymes,
1246 respiratory reference state) is guided by the scientific question under study. Interpretation of
1247 the obtained data depends critically on appropriate normalization, and therefore reporting rates
1248 merely as nmol·s^{-1} is discouraged, since it restricts the analysis to intra-experimental
1249 comparison of relative (qualitative) differences. Expressing O$_2$ consumption per cell may not
1250 be possible when dealing with tissues. For studies with mitochondrial preparations, we
1251 recommend that normalizations be provided as far as possible: (*1*) on a per cell basis as O$_2$ flow
1252 (a biophysical normalization); (*2*) per g cell or tissue protein, or per cell or tissue mass as mass-
1253 specific O$_2$ flux (a cellular normalization); and (*3*) per mitochondrial marker as mt-specific flux
1254 (a mitochondrial normalization). With information on cell size and the use of multiple
1255 normalizations, maximum potential information is available (Renner *et al.* 2003; Wagner *et al.*
1256 2011; Gnaiger 2014).

1257   When using isolated mitochondria, total mitochondrial protein is a frequently applied
1258 mitochondrial marker, the use of which is restricted to isolated mitochondria. The
1259 mitochondrial recovery and yield, and experimental criteria for evaluation of purity versus
1260 integrity should be reported. Mitochondrial markers—such as citrate synthase activity as an
1261 enzymatic matrix marker—provide a link to the tissue of origin on the basis of calculating the

1262 mitochondrial recovery, *i.e.*, the fraction of mitochondrial marker obtained from a unit mass of
1263 tissue.

1264

Table 8. Terms, symbols, and units.

Term	Symbol	*SI* unit	Links and comments
alternative quinol oxidase	AOX		Fig. 1
amount of substance B	n_B	[mol]	
apparent equilibrium constant	K_m'		
Complexes I to IV	CI to CIV		respiratory ET Complexes; Fig. 1
concentration of substance B	$c_B = n_B \cdot V^{-1}$; [B]	[mol·m^{-3}]	Box 2
electron transfer system	ETS		
flow, for substance B	I_B	[mol·s^{-1}]	system-related extensive quantity; Fig. 8
flux, for substance B	J_B	*varies*	size-specific quantitiy; Fig. 8
inorganic phosphate	P_i		
LEAK	LEAK		Tab. 1
mass of sample X	m_X	[kg]	Tab. 4
mass of entity X	M_X	[kg]	Tab. 4
MITOCARTA			https://www.broadinstitute.org/scientific-community/science/programs/metabolic-disease-program/publications/mitocarta/mitocarta-in-0
mitochondria or mitochondrial	mt		Box 1
mitochondrial DNA	mtDNA		Box 1
mitochondrial concentration	$C_{mtE} = mtE \cdot V^{-1}$	[mtEU·m^{-3}]	Tab. 4
mitochondrial content	$mtE_X = mtE \cdot N_X^{-1}$	[mtEU·x^{-1}]	Tab. 4
mitochondrial elemental unit	mtEU	*varies*	Tab. 4, specific units for mt-marker
mitochondrial inner membrane	mtIM		MIM is widely used, and M is replaced by mt as abbreviation for mitochondria; Box 1
mitochondrial outer membrane	mtOM		MOM is widely used, and M is replaced by mt as abbreviation for mitochondria; Box 1
mitochondrial recovery	Y_{mtE}		Fig. 9
mitochondrial yield	$Y_{mtE/m}$		Fig. 9
negative	neg		Fig. 2
number concentration of X	C_{NX}	[x·m^{-3}]	Tab. 4
number of entities X	N_X	[x]	Tab. 4, Fig. 10
number of entity B	N_B	[x]	Tab. 4
oxidative phosphorylation	OXPHOS		Tab. 1
oxygen concentration	$c_{O2} = n_{O2} \cdot V^{-1}$; [O$_2$]	[mol·m^{-3}]	Section 3.2
phosphorylation of ADP to ATP	P»		Section 2.2
positive	pos		Fig. 2
proton in the negative compartment	H^+_{neg}		Fig. 2
proton in the positive compartment	H^+_{pos}		Fig. 2
rate of electron transfer in ET state	E		ET-capacity; Tab. 1
rate of LEAK respiration	L		Tab. 1
rate of oxidative phosphorylation	P		OXPHOS capacity; Tab. 1
rate of residual oxygen consumption	Rox		Tab. 1
residual oxygen consumption	ROX		Tab. 1
specific mitochondrial density	$D_{mtE} = mtE \cdot m_X^{-1}$	[mtEU·kg^{-1}]	Tab. 7
volume	V	[m^{-3}]	
weight, dry weight	W_d	[kg]	used as mass of sample X; Fig. 8
weight, wet weight	W_w	[kg]	used as mass of sample X; Fig. 8

1321

Terms and symbols are summarized in **Table 8**. Their use will facilitate transdisciplinary communication and support further developments towards a consistent theory of bioenergetics and mitochondrial physiology.

Box 3: Mitochondrial and cell respiration

Mitochondrial and cell respiration is the process of exergonic and exothermic energy transformation in which scalar redox reactions are coupled to vectorial ion translocation across a semipermeable membrane, which separates the small volume of a bacterial cell or mitochondrion from the larger volume of its surroundings. The electrochemical exergy can be partially conserved in the phosphorylation of ADP to ATP or in ion pumping, or dissipated in an electrochemical short-circuit. Respiration is thus clearly distinguished from fermentation as the counterpart of cellular core energy metabolism. Respiration is separated in mitochondrial preparations from the partial contribution of fermentative pathways of the intact cell. Residual oxygen consumption—as measured after inhibition of mitochondrial electron transfer—does not belong to the class of catabolic reactions and is, therefore, subtracted from total oxygen consumption to obtain baseline-corrected respiration.

---

5. References

Altmann R (1894) Die Elementarorganismen und ihre Beziehungen zu den Zellen. Zweite vermehrte Auflage. Verlag Von Veit & Comp, Leipzig:160 pp.
Beard DA (2005) A biophysical model of the mitochondrial respiratory system and oxidative phosphorylation. PLoS Comput Biol 1(4):e36.
Benda C (1898) Weitere Mitteilungen über die Mitochondria. Verh Dtsch Physiol Ges:376-83.
Birkedal R, Laasmaa M, Vendelin M (2014) The location of energetic compartments affects energetic communication in cardiomyocytes. Front Physiol 5:376.
Breton S, Beaupré HD, Stewart DT, Hoeh WR, Blier PU (2007) The unusual system of doubly uniparental inheritance of mtDNA: isn't one enough? Trends Genet 23:465-74.
Brown GC (1992) Control of respiration and ATP synthesis in mammalian mitochondria and cells. Biochem J 284:1-13.
Calvo SE, Klauser CR, Mootha VK (2016) MitoCarta2.0: an updated inventory of mammalian mitochondrial proteins. Nucleic Acids Research 44:D1251-7.
Calvo SE, Julien O, Clauser KR, Shen H, Kamer KJ, Wells JA, Mootha VK (2017) Comparative analysis of mitochondrial N-termini from mouse, human, and yeast. Mol Cell Proteomics 16:512-23.
Campos JC, Queliconi BB, Bozi LHM, Bechara LRG, Dourado PMM, Andres AM, Jannig PR, Gomes KMS, Zambelli VO, Rocha-Resende C, Guatimosim S, Brum PC, Mochly-Rosen D, Gottlieb RA, Kowaltowski AJ, Ferreira JCB (2017) Exercise reestablishes autophagic flux and mitochondrial quality control in heart failure. Autophagy 13:1304-317.
Canton M, Luvisetto S, Schmehl I, Azzone GF (1995) The nature of mitochondrial respiration and discrimination between membrane and pump properties. Biochem J 310:477-81.
Chance B, Williams GR (1955a) Respiratory enzymes in oxidative phosphorylation. I. Kinetics of oxygen utilization. J Biol Chem 217:383-93.
Chance B, Williams GR (1955b) Respiratory enzymes in oxidative phosphorylation: III. The steady state. J Biol Chem 217:409-27.
Chance B, Williams GR (1955c) Respiratory enzymes in oxidative phosphorylation. IV. The respiratory chain. J Biol Chem 217:429-38.

Chance B, Williams GR (1956) The respiratory chain and oxidative phosphorylation. Adv Enzymol Relat Subj Biochem 17:65-134.

Cobb LJ, Lee C, Xiao J, Yen K, Wong RG, Nakamura HK, Mehta HH, Gao Q, Ashur C, Huffman DM, Wan J, Muzumdar R, Barzilai N, Cohen P (2016) Naturally occurring mitochondrial-derived peptides are age-dependent regulators of apoptosis, insulin sensitivity, and inflammatory markers. Aging (Albany NY) 8:796-809.

Cohen ER, Cvitas T, Frey JG, Holmström B, Kuchitsu K, Marquardt R, Mills I, Pavese F, Quack M, Stohner J, Strauss HL, Takami M, Thor HL (2008) Quantities, units and smbols in physical chemistry, IUPAC Green Book, 3rd Edition, 2nd Printing, IUPAC & RSC Publishing, Cambridge.

Cooper H, Hedges LV, Valentine JC, eds (2009) The handbook of research synthesis and meta-analysis. Russell Sage Foundation.

Coopersmith J (2010) Energy, the subtle concept. The discovery of Feynman's blocks from Leibnitz to Einstein. Oxford University Press:400 pp.

Cummins J (1998) Mitochondrial DNA in mammalian reproduction. Rev Reprod 3:172-82.

Dai Q, Shah AA, Garde RV, Yonish BA, Zhang L, Medvitz NA, Miller SE, Hansen EL, Dunn CN, Price TM (2013) A truncated progesterone receptor (PR-M) localizes to the mitochondrion and controls cellular respiration. Mol Endocrinol 27:741-53.

Divakaruni AS, Brand MD (2011) The regulation and physiology of mitochondrial proton leak. Physiology (Bethesda) 26:192-205.

Doerrier C, Garcia-Souza LF, Krumschnabel G, Wohlfarter Y, Mészáros AT, Gnaiger E (2018) High-Resolution FluoRespirometry and OXPHOS protocols for human cells, permeabilized fibres from small biopsies of muscle and isolated mitochondria. Methods Mol. Biol. (in press)

Doskey CM, van 't Erve TJ, Wagner BA, Buettner GR (2015) Moles of a substance per cell is a highly informative dosing metric in cell culture. PLOS ONE 10:e0132572.

Drahota Z, Milerová M, Stieglerová A, Houstek J, Ostádal B (2004) Developmental changes of cytochrome *c* oxidase and citrate synthase in rat heart homogenate. Physiol Res 53:119-22.

Duarte FV, Palmeira CM, Rolo AP (2014) The role of microRNAs in mitochondria: small players acting wide. Genes (Basel) 5:865-86.

Ernster L, Schatz G (1981) Mitochondria: a historical review. J Cell Biol 91:227s-55s.

Estabrook RW (1967) Mitochondrial respiratory control and the polarographic measurement of ADP:O ratios. Methods Enzymol 10:41-7.

Faber C, Zhu ZJ, Castellino S, Wagner DS, Brown RH, Peterson RA, Gates L, Barton J, Bickett M, Hagerty L, Kimbrough C, Sola M, Bailey D, Jordan H, Elangbam CS (2014) Cardiolipin profiles as a potential biomarker of mitochondrial health in diet-induced obese mice subjected to exercise, diet-restriction and ephedrine treatment. J Appl Toxicol 34:1122-9.

Fell D (1997) Understanding the control of metabolism. Portland Press.

Garlid KD, Beavis AD, Ratkje SK (1989) On the nature of ion leaks in energy-transducing membranes. Biochim Biophys Acta 976:109-20.

Garlid KD, Semrad C, Zinchenko V. Does redox slip contribute significantly to mitochondrial respiration? In: Schuster S, Rigoulet M, Ouhabi R, Mazat J-P, eds (1993) Modern trends in biothermokinetics. Plenum Press, New York, London:287-93.

Gerö D, Szabo C (2016) Glucocorticoids suppress mitochondrial oxidant production via upregulation of uncoupling protein 2 in hyperglycemic endothelial cells. PLoS One 11:e0154813.

Gnaiger E. Efficiency and power strategies under hypoxia. Is low efficiency at high glycolytic ATP production a paradox? In: Surviving Hypoxia: Mechanisms of Control and Adaptation. Hochachka PW, Lutz PL, Sick T, Rosenthal M, Van den Thillart G, eds (1993a) CRC Press, Boca Raton, Ann Arbor, London, Tokyo:77-109.

Gnaiger E (1993b) Nonequilibrium thermodynamics of energy transformations. Pure Appl Chem 65:1983-2002.

Gnaiger E (2001) Bioenergetics at low oxygen: dependence of respiration and phosphorylation on oxygen and adenosine diphosphate supply. Respir Physiol 128:277-97.

Gnaiger E (2009) Capacity of oxidative phosphorylation in human skeletal muscle. New perspectives of mitochondrial physiology. Int J Biochem Cell Biol 41:1837-45.

Gnaiger E (2014) Mitochondrial pathways and respiratory control. An introduction to OXPHOS analysis. 4th ed. Mitochondr Physiol Network 19.12. Oroboros MiPNet Publications, Innsbruck:80 pp.

Gnaiger E, Méndez G, Hand SC (2000) High phosphorylation efficiency and depression of uncoupled respiration in mitochondria under hypoxia. Proc Natl Acad Sci USA 97:11080-5.

Greggio C, Jha P, Kulkarni SS, Lagarrigue S, Broskey NT, Boutant M, Wang X, Conde Alonso S, Ofori E, Auwerx J, Cantó C, Amati F (2017) Enhanced respiratory chain supercomplex formation in response to exercise in human skeletal muscle. Cell Metab 25:301-11.

Hinkle PC (2005) P/O ratios of mitochondrial oxidative phosphorylation. Biochim Biophys Acta 1706:1-11.

Hofstadter DR (1979) Gödel, Escher, Bach: An eternal golden braid. A metaphorical fugue on minds and machines in the spirit of Lewis Carroll. Harvester Press:499 pp.

1438 Illaste A, Laasmaa M, Peterson P, Vendelin M (2012) Analysis of molecular movement reveals latticelike
1439   obstructions to diffusion in heart muscle cells. Biophys J 102:739-48.
1440 Jasienski M, Bazzaz FA (1999) The fallacy of ratios and the testability of models in biology. Oikos 84:321-26.
1441 Jepihhina N, Beraud N, Sepp M, Birkedal R, Vendelin M (2011) Permeabilized rat cardiomyocyte response
1442   demonstrates intracellular origin of diffusion obstacles. Biophys J 101:2112-21.
1443 Klepinin A, Ounpuu L, Guzun R, Chekulayev V, Timohhina N, Tepp K, Shevchuk I, Schlattner U, Kaambre T
1444   (2016) Simple oxygraphic analysis for the presence of adenylate kinase 1 and 2 in normal and tumor cells. J
1445   Bioenerg Biomembr 48:531-48.
1446 Klingenberg M (2017) UCP1 - A sophisticated energy valve. Biochimie 134:19-27.
1447 Koit A, Shevchuk I, Ounpuu L, Klepinin A, Chekulayev V, Timohhina N, Tepp K, Puurand M,Truu L, Heck K,
1448   Valvere V, Guzun R, Kaambre T (2017) Mitochondrial respiration in human colorectal and breast cancer
1449   clinical material is regulated differently. Oxid Med Cell Longev 1372640.
1450 Komlódi T, Tretter L (2017) Methylene blue stimulates substrate-level phosphorylation catalysed by succinyl-
1451   CoA ligase in the citric acid cycle. Neuropharmacology 123:287-98.
1452 Lane N (2005) Power, sex, suicide: mitochondria and the meaning of life. Oxford University Press:354 pp.
1453 Larsen S, Nielsen J, Neigaard Nielsen C, Nielsen LB, Wibrand F, Stride N, Schroder HD, Boushel RC, Helge
1454   JW, Dela F, Hey-Mogensen M (2012) Biomarkers of mitochondrial content in skeletal muscle of healthy
1455   young human subjects. J Physiol 590:3349-60.
1456 Lee C, Zeng J, Drew BG, Sallam T, Martin-Montalvo A, Wan J, Kim SJ, Mehta H, Hevener AL, de Cabo R,
1457   Cohen P (2015) The mitochondrial-derived peptide MOTS-c promotes metabolic homeostasis and reduces
1458   obesity and insulin resistance. Cell Metab 21:443-54.
1459 Lee SR, Kim HK, Song IS, Youm J, Dizon LA, Jeong SH, Ko TH, Heo HJ, Ko KS, Rhee BD, Kim N, Han J
1460   (2013) Glucocorticoids and their receptors: insights into specific roles in mitochondria. Prog Biophys Mol
1461   Biol 112:44-54.
1462 Leek BT, Mudaliar SR, Henry R, Mathieu-Costello O, Richardson RS (2001) Effect of acute exercise on citrate
1463   synthase activity in untrained and trained human skeletal muscle. Am J Physiol Regul Integr Comp Physiol
1464   280:R441-7.
1465 Lemieux H, Blier PU, Gnaiger E (2017) Remodeling pathway control of mitochondrial respiratory capacity by
1466   temperature in mouse heart: electron flow through the Q-junction in permeabilized fibers. Sci Rep 7:2840.
1467 Lenaz G, Tioli G, Falasca AI, Genova ML (2017) Respiratory supercomplexes in mitochondria. In: Mechanisms
1468   of primary energy trasduction in biology. M Wikstrom (ed) Royal Society of Chemistry Publishing, London,
1469   UK:296-337.
1470 Margulis L (1970) Origin of eukaryotic cells. New Haven: Yale University Press.
1471 Meinild Lundby AK, Jacobs RA, Gehrig S, de Leur J, Hauser M, Bonne TC, Flück D, Dandanell S, Kirk N,
1472   Kaech A, Ziegler U, Larsen S, Lundby C (2018) Exercise training increases skeletal muscle mitochondrial
1473   volume density by enlargement of existing mitochondria and not de novo biogenesis. Acta Physiol 222,
1474   e12905.
1475 Menshikova EV, Ritov VB, Fairfull L, Ferrell RE, Kelley DE, Goodpaster BH (2006) Effects of exercise on
1476   mitochondrial content and function in aging human skeletal muscle. J Gerontol A Biol Sci Med Sci 61:534-
1477   40.
1478 Menshikova EV, Ritov VB, Ferrell RE, Azuma K, Goodpaster BH, Kelley DE (2007) Characteristics of skeletal
1479   muscle mitochondrial biogenesis induced by moderate-intensity exercise and weight loss in obesity. J Appl
1480   Physiol (1985) 103:21-7.
1481 Menshikova EV, Ritov VB, Toledo FG, Ferrell RE, Goodpaster BH, Kelley DE (2005) Effects of weight loss
1482   and physical activity on skeletal muscle mitochondrial function in obesity. Am J Physiol Endocrinol Metab
1483   288:E818-25.
1484 Miller GA (1991) The science of words. Scientific American Library New York:276 pp.
1485 Mitchell P (1961) Coupling of phosphorylation to electron and hydrogen transfer by a chemi-osmotic type of
1486   mechanism. Nature 191:144-8.
1487 Mitchell P (2011) Chemiosmotic coupling in oxidative and photosynthetic phosphorylation. Biochim Biophys
1488   Acta Bioenergetics 1807:1507-38.
1489 Mogensen M, Sahlin K, Fernström M, Glintborg D, Vind BF, Beck-Nielsen H, Højlund K (2007) Mitochondrial
1490   respiration is decreased in skeletal muscle of patients with type 2 diabetes. Diabetes 56:1592-9.
1491 Mohr PJ, Phillips WD (2015) Dimensionless units in the SI. Metrologia 52:40-7.
1492 Moreno M, Giacco A, Di Munno C, Goglia F (2017) Direct and rapid effects of 3,5-diiodo-L-thyronine (T2).
1493   Mol Cell Endocrinol 7207:30092-8.
1494 Morrow RM, Picard M, Derbeneva O, Leipzig J, McManus MJ, Gouspillou G, Barbat-Artigas S, Dos Santos C,
1495   Hepple RT, Murdock DG, Wallace DC (2017) Mitochondrial energy deficiency leads to hyperproliferation of
1496   skeletal muscle mitochondria and enhanced insulin sensitivity. Proc Natl Acad Sci U S A 114:2705-10.
1497 Paradies G, Paradies V, De Benedictis V, Ruggiero FM, Petrosillo G (2014) Functional role of cardiolipin in
1498   mitochondrial bioenergetics. Biochim Biophys Acta 1837:408-17.

Pesta D, Gnaiger E (2012) High-Resolution Respirometry. OXPHOS protocols for human cells and permeabilized fibres from small biopsies of human muscle. Methods Mol Biol 810:25-58.

Pesta D, Hoppel F, Macek C, Messner H, Faulhaber M, Kobel C, Parson W, Burtscher M, Schocke M, Gnaiger E (2011) Similar qualitative and quantitative changes of mitochondrial respiration following strength and endurance training in normoxia and hypoxia in sedentary humans. Am J Physiol Regul Integr Comp Physiol 301:R1078–87.

Price TM, Dai Q (2015) The role of a mitochondrial progesterone receptor (PR-M) in progesterone action. Semin Reprod Med 33:185-94.

Puchowicz MA, Varnes ME, Cohen BH, Friedman NR, Kerr DS, Hoppel CL (2004) Oxidative phosphorylation analysis: assessing the integrated functional activity of human skeletal muscle mitochondria – case studies. Mitochondrion 4:377-85. Puntschart A, Claassen H, Jostarndt K, Hoppeler H, Billeter R (1995) mRNAs of enzymes involved in energy metabolism and mtDNA are increased in endurance-trained athletes. Am J Physiol 269:C619-25.

Quiros PM, Mottis A, Auwerx J (2016) Mitonuclear communication in homeostasis and stress. Nat Rev Mol Cell Biol 17:213-26.

Reichmann H, Hoppeler H, Mathieu-Costello O, von Bergen F, Pette D (1985) Biochemical and ultrastructural changes of skeletal muscle mitochondria after chronic electrical stimulation in rabbits. Pflugers Arch 404:1-9.

Renner K, Amberger A, Konwalinka G, Gnaiger E (2003) Changes of mitochondrial respiration, mitochondrial content and cell size after induction of apoptosis in leukemia cells. Biochim Biophys Acta 1642:115-23.

Rich P (2003) Chemiosmotic coupling: The cost of living. Nature 421:583.

Rostovtseva TK, Sheldon KL, Hassanzadeh E, Monge C, Saks V, Bezrukov SM, Sackett DL (2008) Tubulin binding blocks mitochondrial voltage-dependent anion channel and regulates respiration. Proc Natl Acad Sci USA 105:18746-51.

Rustin P, Parfait B, Chretien D, Bourgeron T, Djouadi F, Bastin J, Rötig A, Munnich A (1996) Fluxes of nicotinamide adenine dinucleotides through mitochondrial membranes in human cultured cells. J Biol Chem 271:14785-90.

Saks VA, Veksler VI, Kuznetsov AV, Kay L, Sikk P, Tiivel T, Tranqui L, Olivares J, Winkler K, Wiedemann F, Kunz WS (1998) Permeabilised cell and skinned fiber techniques in studies of mitochondrial function in vivo. Mol Cell Biochem 184:81-100.

Salabei JK, Gibb AA, Hill BG (2014) Comprehensive measurement of respiratory activity in permeabilized cells using extracellular flux analysis. Nat Protoc 9:421-38.

Sazanov LA (2015) A giant molecular proton pump: structure and mechanism of respiratory complex I. Nat Rev Mol Cell Biol 16:375-88.

Schneider TD (2006) Claude Shannon: biologist. The founder of information theory used biology to formulate the channel capacity. IEEE Eng Med Biol Mag 25:30-3.

Schönfeld P, Dymkowska D, Wojtczak L (2009) Acyl-CoA-induced generation of reactive oxygen species in mitochondrial preparations is due to the presence of peroxisomes. Free Radic Biol Med 47:503-9.

Schultz J, Wiesner RJ (2000) Proliferation of mitochondria in chronically stimulated rabbit skeletal muscle--transcription of mitochondrial genes and copy number of mitochondrial DNA. J Bioenerg Biomembr 32:627-34.

Simson P, Jepihhina N, Laasmaa M, Peterson P, Birkedal R, Vendelin M (2016) Restricted ADP movement in cardiomyocytes: Cytosolic diffusion obstacles are complemented with a small number of open mitochondrial voltage-dependent anion channels. J Mol Cell Cardiol 97:197-203.

Stucki JW, Ineichen EA (1974) Energy dissipation by calcium recycling and the efficiency of calcium transport in rat-liver mitochondria. Eur J Biochem 48:365-75.

Tonkonogi M, Harris B, Sahlin K (1997) Increased activity of citrate synthase in human skeletal muscle after a single bout of prolonged exercise. Acta Physiol Scand 161:435-6.

Waczulikova I, Habodaszova D, Cagalinec M, Ferko M, Ulicna O, Mateasik A, Sikurova L, Ziegelhöffer A (2007) Mitochondrial membrane fluidity, potential, and calcium transients in the myocardium from acute diabetic rats. Can J Physiol Pharmacol 85:372-81.

Wagner BA, Venkataraman S, Buettner GR (2011) The rate of oxygen utilization by cells. Free Radic Biol Med 51:700-712.

Wang H, Hiatt WR, Barstow TJ, Brass EP (1999) Relationships between muscle mitochondrial DNA content, mitochondrial enzyme activity and oxidative capacity in man: alterations with disease. Eur J Appl Physiol Occup Physiol 80:22-7.

Watt IN, Montgomery MG, Runswick MJ, Leslie AG, Walker JE (2010) Bioenergetic cost of making an adenosine triphosphate molecule in animal mitochondria. Proc Natl Acad Sci U S A 107:16823-7.

Weibel ER, Hoppeler H (2005) Exercise-induced maximal metabolic rate scales with muscle aerobic capacity. J Exp Biol 208:1635–44.

White DJ, Wolff JN, Pierson M, Gemmell NJ (2008) Revealing the hidden complexities of mtDNA inheritance. Mol Ecol 17:4925–42.

1561   Wikström M, Hummer G (2012) Stoichiometry of proton translocation by respiratory complex I and its
1562   mechanistic implications. Proc Natl Acad Sci U S A 109:4431-6.
1563   Willis WT, Jackman MR, Messer JI, Kuzmiak-Glancy S, Glancy B (2016) A simple hydraulic analog model of
1564   oxidative phosphorylation. Med Sci Sports Exerc 48:990-1000.